The role of EP300 on regulatory T cells in allergic asthma

Eun Gyul Kim

The Graduate School
Yonsei University
Department of Medical Science

The role of EP300 on regulatory T cells in allergic asthma

A Dissertation Submitted
to the Department of Medical Science
and the Graduate School of Yonsei University
in partial fulfillment of the
requirements for the degree of
Doctor of Philosophy in Medical Science

Eun Gyul Kim

June 2024

This certifies that the Dissertation of Eun Gyul Kim is approved.

Thesis Supervisor Myung Hyun Sohn

Thesis Committee Member Kyung Won Kim

Thesis Committee Member Ho-Geun Yoon

Thesis Committee Member Jae Myun Lee

Thesis Committee Member Tae Won Song

The Graduate School
Yonsei University
June 2024

ACKNOWLEDGEMENTS

4년간의 박사과정을 마치고, 이렇게 한 권의 논문이 나오기까지 저에게 도움을 주신 많은 분들께 감사의 인사를 드립니다.

먼저 실험에 몰두할 수 있도록 아낌없이 지원해 주시고 이끌어 주신 손명현 교수님께 감사 인사드립니다. 부족한 저를 잘 챙겨 주시고, 올바른 방향으로 인도 해 주신 덕분에 무사히 졸업할 수 있었습니다. 그리고 항상 저를 응원해 주시고, 다방면으로 도움 주신 김경원 교수님께도 깊은 감사 드립니다. 저의 논문을 꼼꼼히 살펴봐 주시고, 논문 심사를 통해 더 나은 방향으로 이끌어주신 윤호근 교수님, 이재면 교수님, 송태원 교수님께도 감사드립니다.

학위과정 동안 가족보다 오랜 시간을 함께하며 많은 추억을 쌓은 실험실 식구들에게도 감사 인사드립니다. 저의 인턴 생활부터 박사 졸업까지 모든 과정을 지켜봐 주시면서 항상 따뜻한 말씀 해주시고 격려해 주신 김미나 선생님께 감사 인사드립니다. 그리고 실험적으로 많은 도움 주시고, 지금은 사회에서 자리를 빛내고 계신 홍정연 선생님께 감사합니다. 부족한 선배를 잘 따라주고 열심히 도와준 밝고 배울 점 많은 유진이, 성실하고 꼼꼼한 창현이, 다정하고 사랑스러운 주연이, 세심하고 따뜻한 병찬이와 졸업하여 각자의 위치에서 최선을 다하고 있는 똑 부러지는 지수, 온화한 승민이에게도 고마운 마음을 전합니다.

박사과정을 함께 헤쳐 나가고 있는 범구, 보은, 지수와 각자 멋진 곳에서 일하고 있는 연주, 윤주, 혜진, 그리고 고등학교 열람실에서부터 지금까지 제가 공부하는 걸 지켜본 원희, 소영, 유진이에게도 고맙습니다. 또한, 학위과정 동안 옆에서 희로애락을 함께 하며 저를 든든하게 지켜준 재우에게도 정말 고맙습니다.

제가 공부에 흥미를 느낄 수 있게 도와주신 유승철 선생님, 공태식 선생님, 이유 선생님, 신태양 선생님께도 감사드리며, 지속적인 면담을 통해 진로 고민을 함께해 주셨던 이영미 교수님과 기장서 교수님께 감사의 말씀을 전합니다.

그리고 무엇보다 제가 지금까지 공부할 수 있도록 응원해 주시고 지원해 주신 부모님께 감사 인사드립니다. 제가 바르게 자랄 수 있도록 조언해 주시고 묵묵하게 지지해 주신 아버지와, 저를 항상 사랑으로 믿어주신 어머니 덕분에 행복하게 학위를 마칠 수 있었습니다. 제가 지금 이 자리에 있을 수 있도록 해 주신 모든 것에 대해 깊은 감사를 드립니다. 부모님의 희생 잊지 않고 평생 보답하며 살겠습니다. 그 어느 때보다 힘든 시기를 이겨내고 있는 우리 가족이 나중에 이 글을 보면서 '그땐 그랬지'라고 웃으며 이야기할 수 있는 날이 빠르게 왔으면 좋겠습니다.

마지막으로 저를 도와주신 모든 분께 다시 한번 진심으로 감사드립니다. 이 마음 잊지 않고, 베풀어 주신 마음에 보답할 수 있는 사람이 되도록 노력하겠습니다.

2024년 7월
김은결

TABLE OF CONTENTS

LIST OF FIGURES

LIST OF TABLES

Abstract

The role of EP300 on regulatory T cells in allergic asthma

Background: Asthma is a common chronic inflammatory airway disease and can be modulated via histone acetylation, an epigenetic modification. E1A binding protein p300 (EP300) is a pivotal histone acetyltransferase (HAT) that regulates the transcription of diverse genes involved in multiple signaling pathways and biological processes. This study aimed to confirm the role of EP300 in the development of asthma.

Methods: An allergen-induced asthma model was established in mice with systemic EP300 deletion and Treg cell-specific EP300 deletion. HAT activity and EP300 expression were analyzed after asthma induction. EP300 expression was also evaluated in biopsy samples from patients with asthma and from control subjects. Next, immune responses of T helper 2 cells and regulatory T (Treg) cells were investigated, and functional studies of Treg cells were performed via suppression and differentiation assays. Furthermore, chromatin immunoprecipitation and RNA-sequencing were conducted using the sorted Treg cells. Lastly, the Treg cell proliferation experiment was performed with an EP300 inhibitor, small interfering RNA targeting guanylate binding protein 5 (GBP5), and GBP5 lentiviral overexpression vector.

Results: HAT activity and EP300 levels were elevated in mice with asthma. EP300 expression was also higher in patients with asthma than in control subjects. Mice with systemic EP300 deletion resulted in elevated airway hyperresponsiveness, inflammatory cell numbers, IgE levels, type 2 cytokine production, and severity of inflammation in lung tissues compared with control mice. However, Treg cell-related gene expression and Treg cell population were significantly decreased in mice with systemic EP300 deletion than in the control mice. Functional studies of Treg cells showed that EP300 deletion reduced the suppression ability and differentiation potential of Treg cells. Mice with Treg cell-specific

EP300 deletion also showed exacerbated allergic inflammatory responses, similar to mice with whole-body EP300 deletion. Finally, chromatin immunoprecipitation and RNA-sequencing revealed that *GBP5* was a primary target gene of EP300 in Treg cells. Consequently, the Treg cell proliferation assay confirmed that EP300 regulated Treg cell proliferation via GBP5 activation.

Conclusion: EP300 plays a protective role in the pathogenesis of allergic asthma by regulating Treg cell function. These findings suggest a significance of EP300 in asthma and the possibility of the development of a novel approach to the diagnosis and treatment of asthma.

Key words : asthma, GBP5, EP300, regulatory T cell, T helper 2 cell

1. Introduction

Asthma is a chronic inflammatory disease that affects over 300 million people worldwide, with a continuous increase in the incidence rates in many countries.[1] It is initiated upon recognition of allergens, and allergen-specific T cells induce T helper 2 (Th2) cell differentiation. Th2 cells produce type 2 cytokines, such as IL-4, IL-5, and IL-13, leading to the accumulation of large numbers of eosinophils in the airways. Infiltrated and activated eosinophils and other inflammatory substances stimulate B cells that produce allergen-specific IgE.[2,3] These responses result in airway hyperresponsiveness, airway remodeling, mucus hypersecretion, goblet cell hyperplasia, and a strong Th2 immune reaction.[4,5] The asthma phenotype can be exacerbated by a wide range of triggers, including environmental risk factors, genetic factors, and epigenetic modifications.[6,7] Although various asthma phenotypes have been described clinically and biologically, the pathogenesis of asthma remains unelucidated.[8]

When allergens stimulate the differentiation from naive $CD4^+$ T cells into Th2 cells, they also promote cell differentiation to regulatory T (Treg) cells. Treg cells are characterized by intracellular expression of Foxp3 and mainly secrete a variety of key regulatory cytokines, including TGF-β and IL-10, which suppress Th-driven immune cell responses.[9,10] In recent years, Treg cells have been shown to play a central role in maintaining homeostasis of the cellular immune responses to prevent inflammatory diseases. Moreover, the therapeutic potential of Treg cells, which play an important role in immunosuppression and recovery of inflamed airways in allergic asthma, has been demonstrated in several preclinical and clinical studies.[11] Therefore, the inability of Treg cells to effectively suppress excessive Th2 inflammatory responses may exacerbate allergic asthma.[12]

Epigenetic modifications including acetylation, methylation, and noncoding RNA action are also closely associated with allergic inflammatory disorders such as asthma and rhinitis.[13,14] Histone acetylation is a central epigenetic modification that relaxes chromatin structure by adding an acetyl group *to lysine residues in the* N-terminal tail *of histone* proteins. It is involved in regulating the polarization of naïve T cells into various effector T cells such as Th1, Th2, and Treg cells. Hence, the risk of disease development can be modified by modulating the developmental function of these T cell populations via histone acetylation.[15,16] Histone

acetylation is regulated by histone acetyltransferases (HATs), which can be reversed by histone deacetylases (HDACs). E1A binding protein p300 (EP300) is one of the central HATs and plays a pivotal role in recruiting transcriptional enhancers and regulating gene expressions to control diverse basic cellular processes such as proliferation and homeostasis. [17,18] Dysregulation of EP300 is involved in the development of numerous diseases, including cancer, neurodegenerative disease, and inflammatory diseases.[19-22] EP300-induced histone acetylation plays a crucial role in the Th2 polarization and regulation of Foxp3 expression and Treg cell stability.[23,24] The pathogenesis of asthma is closely associated with histone acetylation, but the specific role of EP300 and the associated mechanism in allergic asthma remain unclear.

This study hypothesized that EP300 might play an important role in allergic asthma by involved in regulating Th2 inflammation. To investigate these, EP300 levels were confirmed in mouse models of allergen-induced asthma and in asthma patients. Next, inflammatory responses were compared between whole-body or cell-specific EP300 deletion mice and control mice. Lastly, chromatin immunoprecipitation-sequencing (ChIP-Seq) and RNA-sequencing (RNA-Seq) were performed to investigate the EP300 target genes and the mechanism of EP300 involved in asthma. This research aimed to investigate the pathophysiological roles of EP300 in asthma and to provide a theoretical basis for EP300 as a new treatment strategy for asthma patients.

2. Materials and methods

2.1. Human Subjects

Transbronchial lung biopsy samples were provided by the Biobank of Soonchunhyang University Bucheon Hospital, a member of the Korea Biobank Network (KBN_A06). Two samples each from patients with asthma and control subjects were included in the study. This study was approved by the ethical committee of the institutional review board of Severance Hospital (IRB No. 4-2023-1122).

2.2. Mice

$EP300^{fl/fl}$, R26-CreERT2, $Foxp3^{DTR\text{-}GFP}$, and $Foxp3^{eGFP\text{-}Cre\text{-}ERT2}$ mice were purchased from The Jackson Laboratory (Bar Harbor, ME, USA). $EP300^{fl/fl}$ mice were crossbred with R26-CreERT2 mice to develop mice with inducible systemic EP300 deletion, and $EP300^{fl/fl}$ mice were also crossbred with $Foxp3^{eGFP\text{-}Cre\text{-}ERT2}$ mice to generate the mice with selective deletion of EP300 in Foxp3-specific cells. Mice were housed in specific-pathogen-free conditions, with a controlled temperature at 23 ± 2 °C and humidity under a 12-hour-light/12-hour-dark cycle with *ad libitum* access to food and tap water. All experimental mice had a C57BL/6 background, and animal studies were approved by the Institutional Animal Care and Use Committee of Yonsei University (IACUC No. 2022-0072).

2.3. Animal models

To induce deletion of EP300, sex- and age-matched five- to seven-week-old mice were intraperitoneally injected with 2 mg of tamoxifen reconstituted in 100 μl of corn oil (both Sigma-Aldrich, St. Louis, MO, USA) once a day for a total of three days. After seven days following the final tamoxifen injection, mice were treated with ovalbumin (OVA; Chicken egg white albumin; Sigma-Aldrich) or house dust mite (HDM; *Dermatophagoides pteronyssinus*; Greer, Lenoir, NC, USA) to induce asthma. For treatment of OVA, mice were intraperitoneally sensitized twice at a two-week interval with 100 μg of OVA and 2 mg of alum (Imject Alum Adjuvant; Thermo Fisher Scientific, Waltham, MA, USA) in phosphate-buffered saline (PBS;

Hyclone Laboratories, Logan, UT, USA). Two weeks after the last sensitization, mice were intranasally challenged daily for three days with 50 μg of OVA in PBS. For treatment of HDM, mice were intraperitoneally sensitized with 10 μg of HDM and 2 mg of alum in PBS on days 0 and 5. Subsequently, mice were intranasally challenged on days 12, 13, and 14 with 50 μg of HDM in PBS. One day after the last challenge, airway hyperresponsiveness was measured. Bronchoalveolar lavage fluid (BALF) and blood samples were collected, and the lungs, spleen, and draining lymph nodes (dLNs) of mice were harvested for further experiments.

2.4. Histone acetyltransferase (HAT) activity assay

The HAT activity of the lungs was assessed by a colorimetric HAT activity assay kit (Abcam, Cambridge, UK) according to the manufacturer's protocol. Briefly, lung tissues were homogenized, and total proteins were extracted using a SDS lysis buffer supplemented with a protease inhibitor cocktail (Thermo Fisher Scientific). The total proteins in lung lysates were quantified using a Pierce™ BCA Protein Assay Kit (Thermo Fisher Scientific). Then, histone H3 pre-coated 96-well plates were incubated with 50 μg of lung tissue lysates and HAT reaction mixture at 37 °C for 4 hours. The absorbance was measured at 440 nm by a microplate reader (Molecular Devices, San Jose, CA, USA).

2.5. Western blot analysis

A total of 20 μg of lung protein samples were run on to 4–20% precast polyacrylamide gel (Bio-Rad Laboratories, Inc., Hercules, CA, USA) and then electrophoretically transferred to a polyvinylidene difluoride membrane (Millipore, Bedford, MA, USA). Subsequently, the membrane was washed and blocked with 5% skimmed milk (Becton Dickinson, Sparks, MD, USA) for 1 hour and incubated overnight at 4 °C with specific primary antibodies against anti-EP300 (Abcam, Cambridge, UK) and anti-β-actin (Cell Signaling Technology, Danvers, MA, USA). The next day, the membranes were incubated for 1 hour at room temperature with horseradish peroxidase-conjugated anti-rabbit secondary antibody (Santa Cruz Biotechnology, Dallas, TX, USA) and visualized using an ImageQuant™ LAS4000 Mini Biomolecular Imager (GE Healthcare, Buckinghamshire, UK) with an enhanced chemiluminescent substrate (Thermo Scientific). The Image J software (1.52a; Java 1.8.0 version; National Institutes of Health, Bethesda, MD, USA) was used for densitometric analysis.

2.6. Immunohistochemistry (IHC) staining and histological analysis

To observe the expression of EP300, IHC staining was conducted in mouse and human lung samples. All reagents for IHC staining were purchased from Dako (Glostrup, Denmark) unless otherwise stated. Mouse and human paraffin sections were deparaffinized with xylene and rehydrated with ethyl alcohol. Sections were then heated by antigen retrieval buffer with a boiling steamer for 20 minutes, followed by a cool-down at room temperature for 30 minutes. The sections were incubated with a peroxidase-blocking reagent and protein-blocking solution and then subjected to an anti-EP300 antibody (Abcam). The next day, tissue sections were incubated with the labeled polymer followed by incubation with DAB chromogen-substrate solution for 15 minutes and then mounted with an aqueous mounting medium. Histological images were acquired using an Olympus BX43 Upright Microscope (Olympus, Tokyo, Japan). The Image J software was used for the calculation of EP300 intensity in human samples. To observe histological injury, paraffin-embedded mouse lung specimens were cut into 4 μm sections and stained with hematoxylin and eosin (H&E) or periodic acid-Schiff (PAS) stain.

2.7. Complete blood count (CBC) analysis

Seven days after the final tamoxifen treatment, whole blood samples were collected via retro-orbital bleeding technique from $EP300^{+/+}$ and $EP300^{\Delta/\Delta}$ mice or Foxp3-$EP300^{+/+}$ and Foxp3-$EP300^{\Delta/\Delta}$ mice. A CBC was conducted using a HEMAVET 950 (Drew Scientific, Oxford, CT, USA).

2.8. Measurement of airway hyperresponsiveness

Mice were anesthetized with zoletil (Virbac, Carros, France) and rompun (Bayer, Leverkusen, Germany), and their tracheas were cannulated by tracheostomy with ligation, followed by an assessment of airway-specific resistance with a FlexiVent^{TM} FX 1 apparatus (SCIREQ, Montreal, Canada) using a single-compartment (“snapshot”) perturbation. Respiratory frequency was set at 150 breaths per minute, and a positive end-expiratory pressure (3 cm H_2O) was applied. The mice inhaled normal saline and methacholine aerosol (3.125, 6.25, 12.5, 25, and 50 mg/mL). Assessments were performed at least three times per dose, and the average was calculated.

2.9. Bronchoalveolar lavage fluid (BALF) cell collection and count

The trachea was exposed, and BALF was obtained via a catheter inserted into the exposed trachea following the instillation of PBS. BALF was centrifuged (5 min, 800 × *g*, 4 °C), and the supernatant was frozen. Total cell count was evaluated using a hemocytometer and differential cell count was examined after Diff-Quick staining (PanReac AppliChem, Darmstadt, Germany).

2.10. Enzyme-linked immunosorbent assay (ELISA)

The concentrations of total IgE in the serum were measured by OptEIA™ IgE ELISA Set (BD biosciences, San Diego, CA, USA) according to the manufacturer's protocol. OVA-specific IgE ELISA was performed with slight modifications to the protocol. Briefly, 96-well plates were coated with OVA and blocked with fetal bovine serum (FBS; Corning Inc, Corning, NY, USA). Diluted standards and samples were loaded and detected with anti-mouse IgE antibody and streptavidin-horseradish peroxidase. The plates were developed with tetramethylbenzidine (KPL, Gaithersburg, MD, USA), and the reaction was stopped with 2 N sulfuric acid. The absorbance was measured using a microplate reader at 450 nm wavelength. IL-4, 5, and 13 levels in BALF were quantified by DuoSet ELISA (R&D Systems, Minneapolis, MN, USA) according to the manufacturer’s instructions.

2.11. RNA isolation and real-time PCR analysis

Total RNA was extracted from the lungs and Treg cells in the lung and spleen using TRIzol™ Reagent (Invitrogen, Carlsbad, CA, USA), according to the manufacturer's instructions. cDNA was prepared from the RNA by ReverTra Ace® qPCR RT Master Mix Kit (Toyobo Co., Ltd., Osaka, Japan), and quantitative real-time PCR was performed using StepOnePlus™ Real-Time PCR System (Applied Biosystems, Foster City, CA, USA) with Power SYBR Green® PCR Master Mix (Applied Biosystems). Relative amounts of mRNA were normalized to β-actin levels and calculated according to the comparative Ct ($2^{-\Delta\Delta Ct}$) method.

2.12. Isolation of lymphocytes

Lungs were cut and digested for 1 hour in PBS with collagenase II (300 U/mL; Worthington Biochemicals, Lakewood Township, NJ, USA) and DNase I (150 μg/mL; Roche Applied Science, Mannheim, Germany) at 37 °C. Digested lungs and harvested spleen and dLNs were filtered through a 40 μm cell strainer (BD Biosciences) with RPMI 1640 medium (Hyclone Laboratories) containing 5% FBS and 1% penicillin-streptomycin (Cytiva, Marlborough, MA, USA). Samples were centrifuged and red blood cells were lysed with ammonium chloride-potassium lysis buffer. Cells were then washed twice and followed by resuspension in RPMI 1640 medium containing 5% FBS and 1% penicillin-streptomycin to count the total cells.

2.13. Flow cytometry analysis

Single-cell suspensions were obtained as described above, and 1–2 × 10^6 cells were stained with fluorescent conjugated antibodies. Antibodies were purchased from eBioscience (San Diego, CA, USA) unless otherwise stated. The following antibodies were used in this study: PerCP-Cy5.5 or PE-conjugated anti-CD4, PE-conjugated anti-Foxp3, and APC-conjugated anti-EP300 (Novus Biologicals, Centennial, CO, USA). Fixable Viability Dye eFluor780 was used for the exclusion of dead cells. Surface staining was performed, and the cells were fixed and permeabilized using a Foxp3/Transcription Factor Staining Buffer Set (eBioscience), followed by intracellular staining. Stained cells were detected by LSR Fortessa™ (BD Biosciences), and the data were analyzed with the FlowJo software (Tree Star, Inc., Ashland, OR, USA).

2.14. *In vitro* Treg cell suppression assay and differentiation assay

For the Treg cell suppression assay, $CD4^+$ $CD25^-$ conventional T (Tconv) cells from the spleen of wild-type (WT) mice and $CD4^+$ $CD25^+$ Treg cells from the spleen of $EP300^{+/+}$ or $EP300^{\Delta/\Delta}$ mice were isolated using a $CD4^+$ $CD25^+$ Regulatory T Cell Isolation Kit (Miltenyi Biotec, Auburn, CA, USA), according to the manufacturer's protocol. Tconv cells (5 × 10^4) were labeled with CellTrace™ CFSE (Invitrogen) and co-cultured with anti-CD3 (1 μg/mL; eBioscience), irradiated (30 Gy) splenocytes (5 × 10^4) as APCs, and varying ratios of Treg cells in 96-well plates. After four days of incubation in an incubator with 5% CO_2 at 37 °C, cells

were harvested, and the proliferation of Tconv cells was analyzed by flow cytometry of CFSE dilution.

For the Treg cell differentiation assay, $CD4^+$ $CD25^-$ T cells from the spleen of $EP300^{+/+}$ or $EP300^{\Delta/\Delta}$ mice were isolated using a $CD4^+$ $CD25^+$ Regulatory T Cell Isolation Kit. $EP300^{+/+}$ or $EP300^{\Delta/\Delta}$ $CD4^+$ $CD25^-$ T cells (2×10^5) were cultured in 96-well plates with anti-CD3 (2 μg/mL), anti-CD28 (1 μg/mL; eBioscience), and rIL-2 (50 ng/mL; ProteinTech Group, Inc., Chicago, Il, USA) in the presence or absence of rTGF-β1 (5 ng/mL; R&D systems) for three days. Subsequently, $CD4^+$ $Foxp3^+$ induced Treg (iTreg) cells were assessed by flow cytometry.

2.15. *In vitro* Treg cell proliferation assay

$CD4^+$ T cells from the spleen were isolated using a $CD4^+$ T Cell Isolation Kit (Miltenyi Biotec), according to the manufacturer's instructions. To induce Treg cells, $CD4^+$ T cells were seeded in 100 mm dishes and cultured with anti-CD3 (2 μg/mL), anti-CD28 (1 μg/mL), rIL-2 (50 ng/mL), and rTGF-β1 (10 ng/mL) for three days at 37 °C in an atmosphere containing 5% CO_2. $CD4^+$ $Foxp3^+$ iTreg cells were then sorted using an Aria™ III cell sorter (BD Bioscience).

For small interfering RNA (siRNA) transfection, the sorted iTreg cells were transfected with 75 pM of scrambled or Guanylate Binding Protein 5 (GBP5) siRNA (Santa Cruz Biotechnology) using a Lipofectamine™ 3000 Transfection Reagent (Invitrogen) in six-well plates according to the manufacturer's instructions. One day after transfection, 2×10^5 cells were seeded in 96-well plates and re-stimulated with anti-CD3, anti-CD28, and rIL-2 for three days. Subsequently, the CCK-8 solution (10 μL; Dojindo Molecular Technologies, Rockville, MD, USA) was added to each well and the proliferative capacity of iTreg cells was evaluated by measuring the absorbance at 450 nm using a microplate reader. The remaining iTreg cells were collected for RNA extraction.

For EP300 inhibitor treatment, iTreg cells were sorted and seeded at a density of 2×10^5 in 96-well plates. Subsequently, iTreg cells were re-stimulated with anti-CD3, anti-CD28, and rIL-2 in the presence or absence of C646 (10 μM; Selleck Chemical, Houston, TX, USA) for three days. After stimulation, iTreg cell proliferation was assessed by CCK-8 assay. The remaining iTreg cells were collected for RNA extraction.

For lentivirus (LV) transduction, $CD4^+$ $Foxp3^+$ Treg cells from the spleen were sorted using an Aria™ III cell sorter. The sorted Treg cells were spin-infected (1.5 hours, 1000 × *g*, 32 °C)

with 5 μg/mL of polybrene (Sigma-Aldrich) and control vector LV or GBP5 overexpression vector LV at a MOI of 10 (VectorBuilder, Guangzhou, China). Cells were incubated for 4 hours at 37 °C and cultured for another two days after the fresh medium change. Then, LV-transduced cells were examined using an Olympus IX73 Fluorescent Inverted Microscope (Olympus). Subsequently, 2×10^5 cells in 96-well plates were stimulated with anti-CD3 (2 μg/mL), anti-CD28 (1 μg/mL), and rIL-2 (50 ng/mL) for three days, and Treg cell proliferation was assessed by CCK-8 assay.

2.16. Chromatin immunoprecipitation-sequencing (ChIP-Seq)

$CD4^+$ $Foxp3^+$ Treg cells in the lungs were sorted using an Aria™ III cell sorter. The sorted Treg cells were used for ChIP-seq, which was performed using the CUT&Tag-IT™ Assay Kit (Active Motif, Carlsbad, CA, USA) according to the manufacturer's instructions. Briefly, sorted cells were washed with wash buffer, and then bound to the activated Concanavalin A coated magnetic beads. After the unbound supernatant was removed, the bead-bound cells were incubated overnight with a 1:50 dilution of EP300 or Acetylated Histone H3K9 antibody (both Cell Signaling) on an orbital shaker at 4 °C. A 1:100 dilution of anti-Rabbit IgG secondary antibody was added to the primary antibody-bound magnetic beads. Cells were washed using the magnet stand with wash buffer to remove unbound antibodies. The pA-Tn5 adapter complex was diluted in Dig-300 buffer and then incubated with magnetic beads for 1 hour at room temperature. After washing the unbound complex, bead-bound cells were resuspended in a Tagmentation buffer for 1 hour at 37 °C. To stop tagmentation, 0.5 M EDTA, 10% SDS, and 10 mg/mL Proteinase K were added to the sample, followed by incubation at 55 °C for 1 hour. The labeled DNA fragments were purified with a DNA purification column. Each eluted sample underwent PCR with a combination of indexed primers designed with Illumina Nextera adapters (Illumina, Inc., San Diego, CA, USA) for the preparation of libraries. Libraries were then sequenced with pair-end reads of 150 bp using Illumina NovaSeq (Illumina, Inc.). Peaks in the aligned sequence data were called by model-based analysis of ChIP-Seq (MACS2, version 2.1.1).[25] ChIPseeker (version 1.22.1),[26] a Bioconductor package within R (version 3.6.3) to facilitate batch annotation of enriched peaks, was used to identify nearby genes and transcripts from the peaks obtained from MACS2. Integrative Genomics Viewer (IGV) software was used for the visual exploration of genomic data.

2.17. RNA-sequencing (RNA-Seq)

Total RNA was extracted from the sorted $CD4^+$ $Foxp3^+$ Treg cells in the lungs using a QIAzol® Lysis Reagent and RNeasy® Mini Kit (both QIAGEN Sciences, Inc., Germantown, MD, USA) according to the manufacturer's protocols. RNA-Seq library was prepared using the Illumina TruSeq Stranded mRNA Sample Prep Kit (Illumina, Inc.). Indexed libraries were then sequenced using an Illumina NovaSeq platform with pair-end reads of 100 bp. Reference genome sequence and gene annotation data were downloaded from the NCBI genome assembly and NCBI reference sequence database, respectively. Gene and transcript levels were quantified as raw read count, Fragments Per Kilobase of transcript per Million mapped reads, and Transcripts Per Million. Statistical analysis of differential gene expression was performed via EdgeR (version 3.40.2) using raw counts as input. All *p*-values were adjusted by the Benjamini-Hochberg algorithm to control the false discovery rate, and the list of significant genes was filtered with |fold change| ≥ 1.5 and raw *p*-value < 0.05. Gene ontology (GO) analysis was performed using a Database for Visualization and Integrative Discovery functional analysis software (https://david.ncifcrf.gov).

2.18. Statistical analysis

Student unpaired *t*-tests were used for two-group comparisons. For more than two groups, one-way ANOVA, followed by Tukey's multiple comparisons test was used. The results of CBC analysis are presented as mean ± standard deviation and other data are presented as mean ± standard error of the mean (SEM). All analyses were performed using the Prism software (8.0 version; Graph-Pad Software, San Diego, CA, USA). A *p*-value of < 0.05 was considered to be statistically significant.

3. Results

3.1. Increased EP300 expression is associated with allergic asthma

To investigate the pathological relevance of EP300 in asthma while avoiding embryonic lethality, $EP300^{fl/fl}$ mice were crossed with R26-CreERT2 mice to develop mice with tamoxifen-inducible EP300 deletion, $EP300^{fl/fl}$;R26-CreERT2 (hereafter, referred to as $EP300^{\Delta/\Delta}$) mice. $EP300^{fl/fl}$ (hereafter, referred to as $EP300^{+/+}$) littermate mice were used as control animals. Mice were intraperitoneally injected with tamoxifen for conditional deletion of EP300. Then, $EP300^{+/+}$ mice and EP300 gene-deleted $EP300^{\Delta/\Delta}$ mice were intraperitoneally and intranasally treated with OVA for the induction of allergic asthma (Fig. 1A). HAT activity was increased in OVA-treated $EP300^{+/+}$ mice than that in PBS-treated $EP300^{+/+}$ mice (Fig. 1B). EP300 protein levels were also significantly increased in OVA-treated $EP300^{+/+}$ mice than those in PBS-treated $EP300^{+/+}$ mice (Fig. 1C, D). IHC staining showed that OVA-induced airway inflammation remarkably increased the EP300 expression in mouse lung cells, including the bronchial epithelial and inflammatory cells (Fig. 1E). Furthermore, tamoxifen treatment induced conditional deletion of EP300 in PBS or OVA-treated $EP300^{\Delta/\Delta}$ mice (Fig. 1C-E). Next, EP300 expression was compared in lung biopsies of non-asthmatic and asthmatic subjects. None of the subjects were smokers, and the clinical characteristics of the subjects are summarized in Table 1. Importantly, the number of EP300-positive cells was significantly higher in the patients with asthma than in control subjects (Fig. 1F, G). These results suggest that aberrant expression of the EP300 in the lung may contribute to allergic inflammation in asthma.

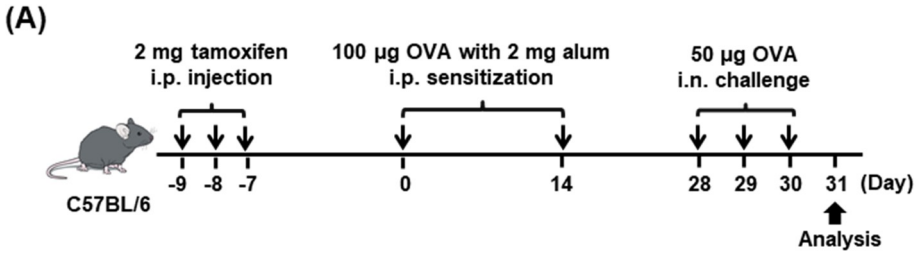

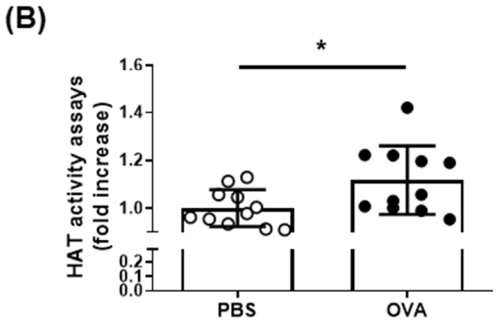

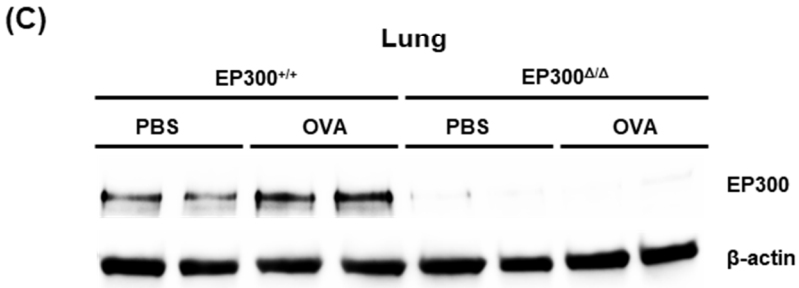

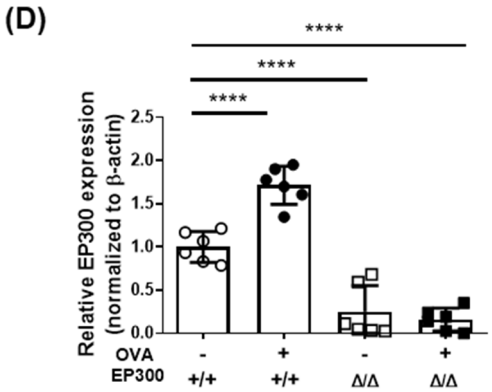

(E)

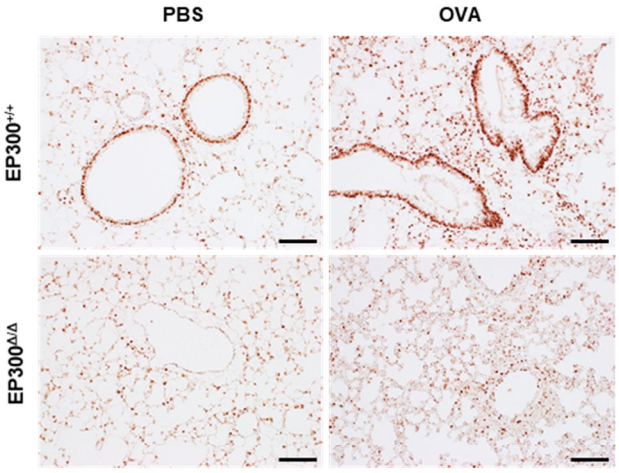

(F)

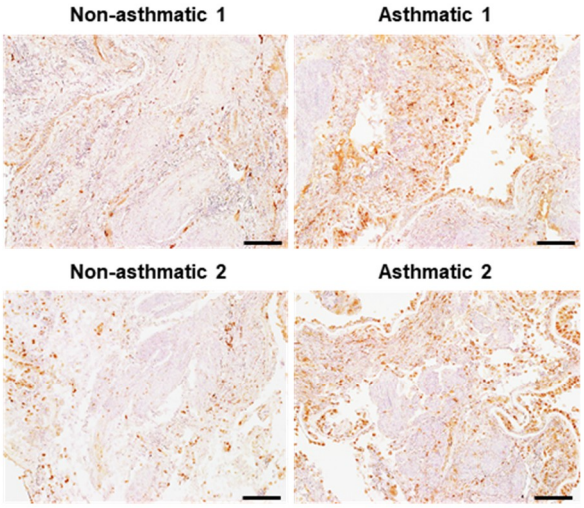

(G)

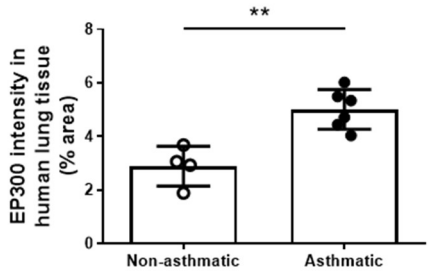

Fig. 1. EP300 levels are elevated in a mouse model of asthma and patients with asthma. (A) A schematic diagram of tamoxifen-induced EP300 deletion and development of a mouse model with OVA-induced allergic asthma. (B) HAT activity was measured in the lungs of $EP300^{+/+}$ mice. (C, D) EP300 protein concentrations in the lungs were analyzed by western blot (C), and signal intensity was quantified by the Image J software (D). (E) Representative images of mouse lung histology were analyzed for EP300 expression by IHC staining. The scale bar indicates 100 μm. (F) Representative images of human lung biopsy were assessed for EP300 expression from non-asthmatic and asthmatic subjects by IHC staining. The scale bar indicates 100 μm. (G) Dot plots represent the EP300 intensity in two fields per non-asthmatic subject and three fields per asthmatic subject determined using the Image J software. The data are presented as the means ± SEM. *p*-values were analyzed by Student's *t*-test and one-way ANOVA with Tukey's multiple comparisons test. $^{*}p < 0.05$; $^{**}p < 0.01$; $^{****}p < 0.0001$.

Table 1. Clinical data of study subjects

	Non-asthmatic subject 1	**Non-asthmatic subject 2**	**Asthmatic subject 1**	**Asthmatic subject 2**
Sex	Female	Female	Male	Female
Age, years	39	39	34	38
FVC, L	3.22	3.3	4.29	3.29
FVC, % predicted	96	102	84	89
FEV_1, L	2.79	2.7	3.18	2.97
FEV_1, % predicted	107	107	80	102
FEV_1/FVC, %	87	82	74	90
Serum IgE, kU/L	-	3.47	47.6	145
BAL eosinophil, %	1.8	0.2	19.6	13.6

FVC, forced vital capacity; FEV_1, forced expiratory volume in 1s; IgE, immunoglobulin E; BAL, bronchoalveolar lavage.

3.2. EP300 regulates airway hyperresponsiveness and allergic inflammation

To confirm the contribution of EP300 in allergic asthma, immune responses were evaluated in $EP300^{+/+}$ and $EP300^{\Delta/\Delta}$ mice after OVA treatment. Before comparison, a CBC analysis was performed to determine any potential differences in basal cell counts between $EP300^{+/+}$ and $EP300^{\Delta/\Delta}$ mice. CBC analysis showed that inflammatory cell populations in $EP300^{+/+}$ and $EP300^{\Delta/\Delta}$ mice were in the normal range and not significantly different between the two groups, confirming the absence of no fundamental defects in $EP300^{\Delta/\Delta}$ mice (Table 2). Subsequently, airway hyperresponsiveness measurement showed that airway resistance was amplified in OVA-treated $EP300^{+/+}$ and OVA-treated $EP300^{\Delta/\Delta}$ mice; however, OVA-treated $EP300^{\Delta/\Delta}$ mice had more amplified airway hyperresponsiveness (Fig. 2A). Next, a greater number of infiltrated cells, especially eosinophils, were observed in $EP300^{\Delta/\Delta}$ mice than those in $EP300^{+/+}$ mice upon OVA treatment (Fig. 2B). Subsequently, the levels of OVA-specific IgE in serum and the expression of Th2 cytokines IL-4, IL-5, and IL-13 in the lungs and BALF were substantially increased in OVA-treated $EP300^{\Delta/\Delta}$ mice relative to those in OVA-treated $EP300^{+/+}$ mice (Fig. 2C-I). Lastly, enhanced inflammatory infiltration (Fig. 2J) and increased goblet cell expansion and mucus production (Fig. 2K) were observed in the lungs of $EP300^{\Delta/\Delta}$ mice compared to those in $EP300^{+/+}$ mice after asthma induction.

Table 2. Summary of CBC analysis for $EP300^{+/+}$ and $EP300^{\Delta/\Delta}$ mice

Blood count parameters	$EP300^{+/+}$ (n = 3)	$EP300^{\Delta/\Delta}$ (n = 3)	Normal range
White blood cells, $10^3/\mu l$	3.56 ± 0.85	3.80 ± 1.54	0.80-10.60
Neutrophils, %	15.3 ± 9.22	17.90 ± 8.09	6.5-50.0
Lymphocytes, %	78.30 ± 8.52	75.73 ± 7.71	40.0-92.0
Monocytes, %	4.07 ± 1.56	4.93 ± 1.40	0.9-18.0
Eosinophils, %	2.33 ± 0.90	1.43 ± 0.06	0.0-7.5
Basophils, %	0.00 ± 0.00	0.00 ± 0.00	0.0-1.5

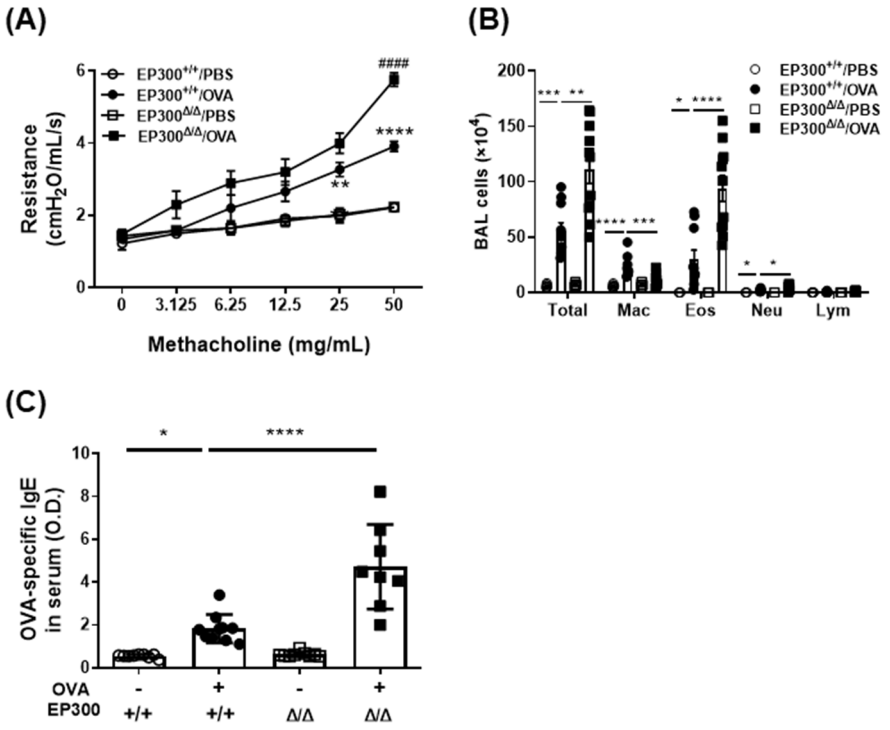

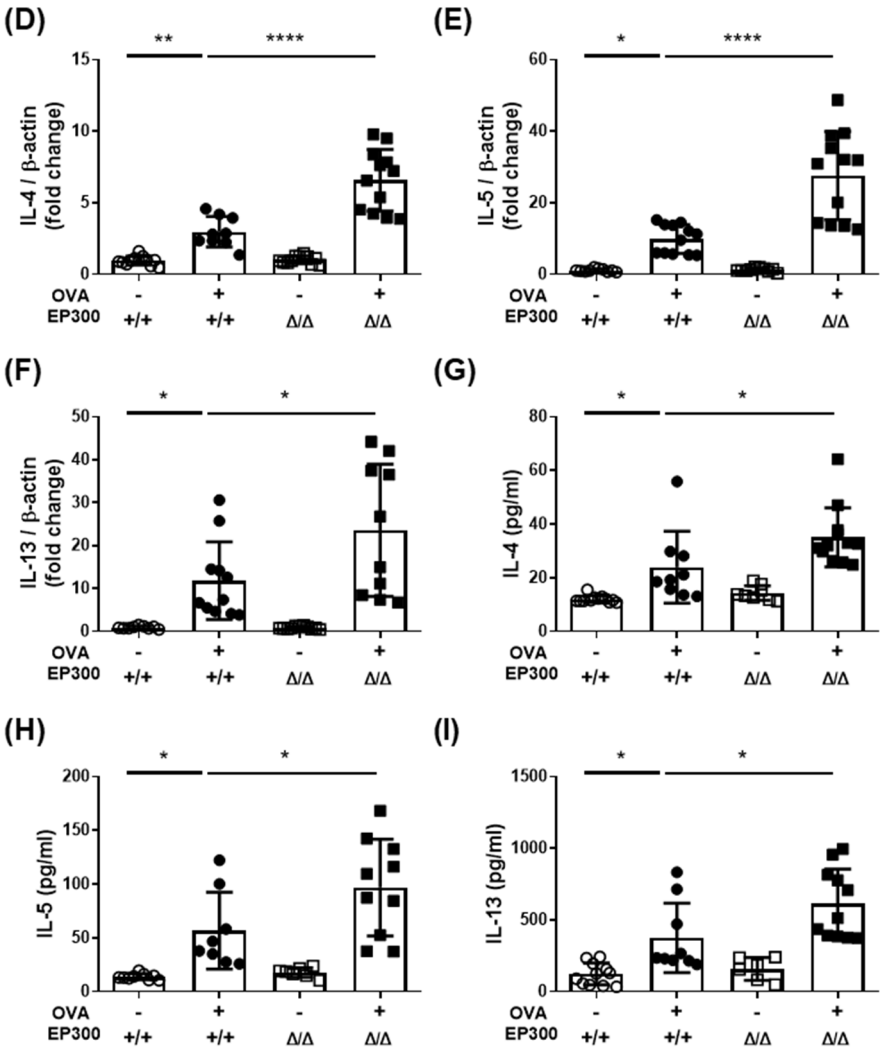

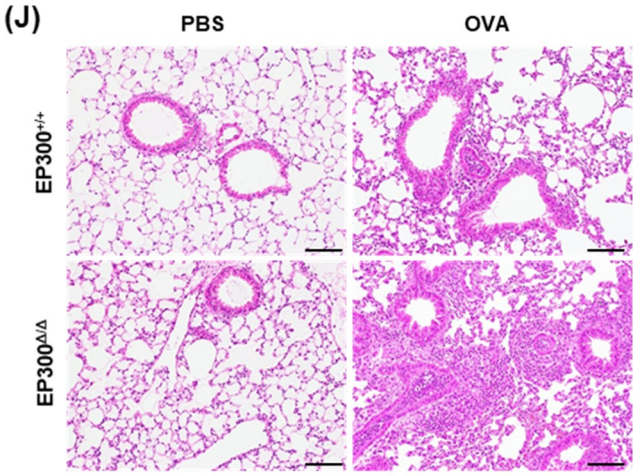

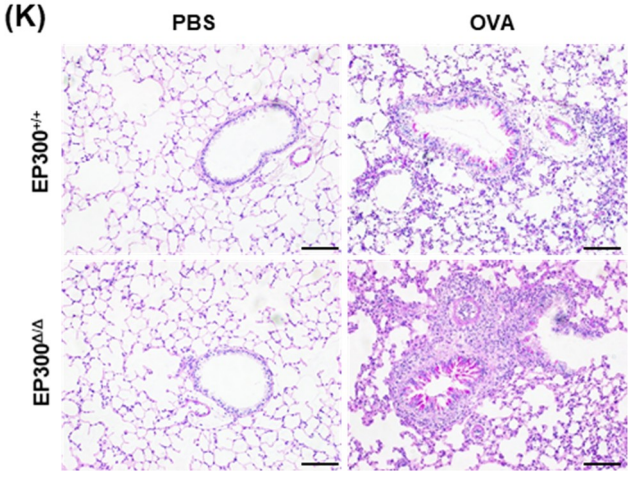

Fig. 2. Conditional deletion of EP300 deteriorates OVA-induced type 2 airway inflammation. (A) Airway resistance in response to increasing doses of methacholine was measured by the FlexiVent system. (B) Total and differential cells in BALF were counted. (C) OVA-specific IgE levels in serum were determined by ELISA. (D-F) mRNA expression levels of IL-4 (D), IL-5 (E), and IL-13 (F) in the lungs were measured by quantitative real-time PCR. (G-I) Protein levels of IL-4 (G), IL-5 (H), and IL-13 (I) in the BALF were quantified by ELISA. (J, K) Representative images of lung histology were analyzed for inflammatory cell infiltrations by H&E staining (J) and mucus production in goblet cells by PAS staining (K). The scale bar indicates 100 μm. The data are presented as the means ± SEM. *p*-values were analyzed by one-way ANOVA with Tukey's multiple comparisons test. $^{*}p < 0.05$; $^{**}p < 0.01$; $^{***}p < 0.001$; $^{****}p < 0.0001$. In figure (A), $^{**}p < 0.01$, $^{****}p < 0.0001$ for $EP300^{+/+}$/PBS vs. $EP300^{+/+}$/OVA and $^{\#\#\#\#}p < 0.0001$ for $EP300^{+/+}$/OVA vs. $EP300^{\Delta/\Delta}$/OVA.

HDM is another allergen of high clinical relevance used in the experimental model of asthma. Hence, HDM-induced airway allergic models were established in $EP300^{+/+}$ and $EP300^{\Delta/\Delta}$ mice (Fig. 3A). Similar to the results in the OVA-induced asthma model, both HAT activity and EP300 protein levels were increased in the lungs after HDM sensitization and challenge (Fig. 3B, C). Moreover, airway resistance, inflammatory cells in BALF, IgE concentration, and histological lung injury, as well as Th2-type cytokine expression were also remarkably elevated in the HDM-treated $EP300^{\Delta/\Delta}$ mice than those in HDM-treated $EP300^{+/+}$ mice (Fig. 3D-J). Therefore, the ablation of EP300 aggravated airway inflammation in the OVA and HDM models.

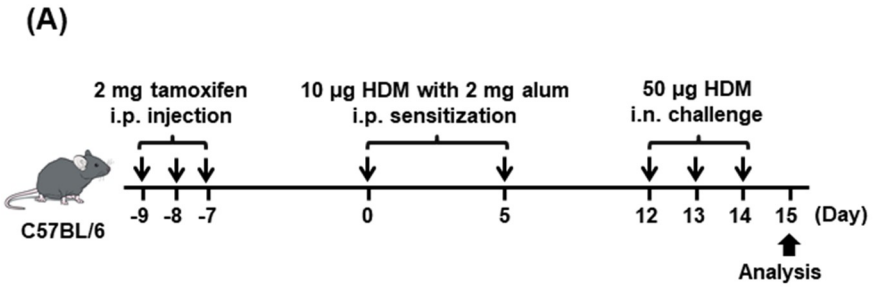

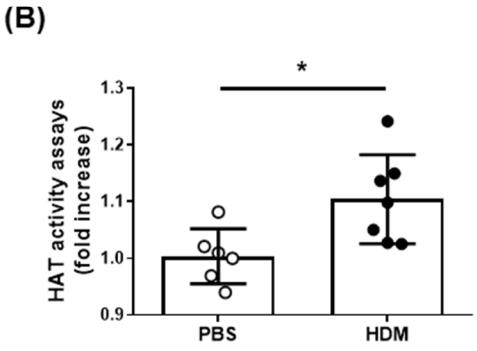

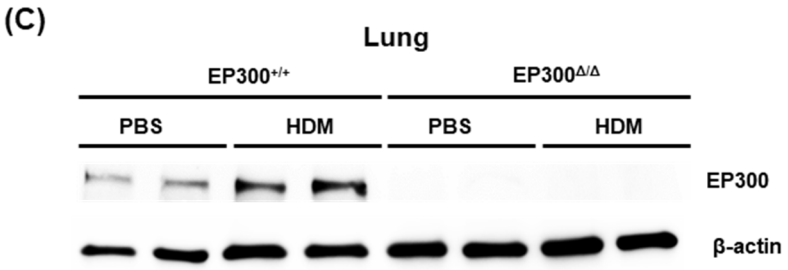

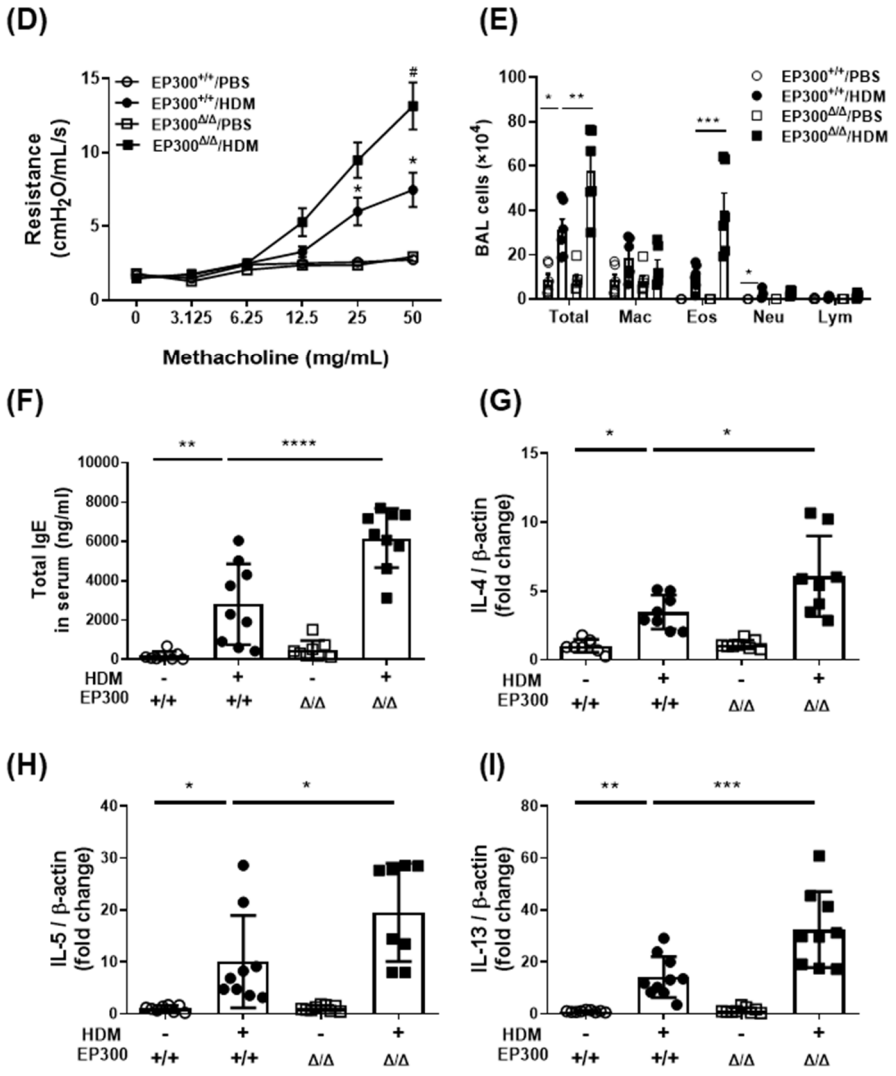

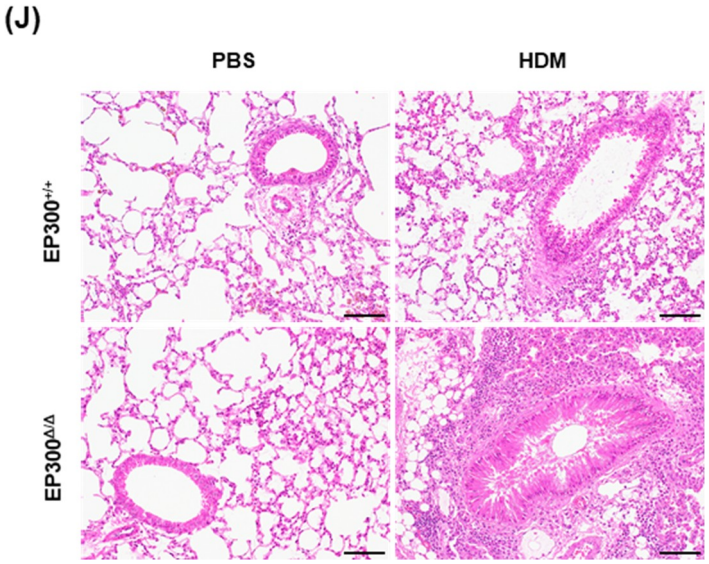

Fig. 3. Conditional deletion of EP300 exacerbates HDM-induced airway hyperresponsiveness and airway inflammation. (A) A protocol of tamoxifen-induced EP300 deletion and HDM-induced allergic asthma in a mouse model. (B) HAT activity was analyzed from the lungs of $EP300^{+/+}$ mice. (C) EP300 protein levels in the lungs were assessed by Western blot. (D) Airway resistance was determined by the FlexiVent system. (E) Total and differential cells in BALF were quantitated. (F) Serum levels of total IgE were measured by ELISA. (G-I) mRNA levels of IL-4 (G), IL-5 (H), and IL-13 (I) in the lungs were evaluated by quantitative real-time PCR. (J) Representative images show lung histological sections stained by H&E. The scale bar indicates 100 μm. The data are presented as the means ± SEM. *p*-values were analyzed by Student's *t*-test and one-way ANOVA with Tukey's multiple comparisons tests. $^{*}p < 0.05$; $^{**}p < 0.01$; $^{***}p < 0.001$; $^{****}p < 0.0001$. In figure (D), $^{*}p < 0.05$ for $EP300^{+/+}$/PBS vs. $EP300^{+/+}$/HDM and $^{\#}p < 0.05$ for $EP300^{+/+}$/HDM vs. $EP300^{\Delta/\Delta}$/HDM.

3.3. EP300 increases Treg cell population and enhances Treg cell function

Asthma is developed by dysregulation of Th2 immune responses and increasing evidence suggests that Treg cells potentially control the Th2-type responses and maintain a state of immune tolerance against allergens.[27] To investigate whether EP300 is involved in Treg cells during the progression of asthma. EP300 levels in Treg cells were confirmed. EP300 expression was increased in Foxp3-positive cells in the lungs upon OVA treatment (Fig. 4A, B). The mRNA expression levels of Treg cell transcription factor Foxp3 and related cytokines IL-10 and TGF-β were significantly elevated in the OVA-treated $EP300^{+/+}$ mice than those in the PBS-treated $EP300^{+/+}$ mice but were attenuated in OVA-treated $EP300^{\Delta/\Delta}$ mice (Fig. 4C-E). Furthermore, regulatory T cell populations in the lungs and spleen were lower in OVA-treated $EP300^{\Delta/\Delta}$ mice than in OVA-treated $EP300^{+/+}$ mice (Fig. 4F-I). To further understand the role of EP300 in the Treg cells, it was confirmed whether EP300 regulated Treg cell functions, such as the ability of Treg cells to suppress T cell proliferation and conversion from naive T cells to Treg cells. First, to evaluate the suppression ability of Treg cells, Treg cells from $EP300^{+/+}$ and $EP300^{\Delta/\Delta}$ mice were co-cultured with WT Tconv cells. $EP300^{\Delta/\Delta}$ Treg cells were impaired in suppressing the proliferation of Tconv cells compared to $EP300^{+/+}$ Treg cells (Fig. 4J). The suppression percentage also indicated that suppression ability was reduced in a ratio-dependent manner in $EP300^{\Delta/\Delta}$ Treg cells than in $EP300^{+/+}$ Treg cells (Fig. 4K). Next, $CD4^+$ $CD25^-$ naive T cells were isolated from $EP300^{+/+}$ and $EP300^{\Delta/\Delta}$ mice and stimulated with rTGF-β1, to evaluate the differentiation potential into iTreg cells. The percentage of iTreg cells in $EP300^{\Delta/\Delta}$ induction groups was significantly lower than that of $EP300^{+/+}$ induction groups ($EP300^{+/+}$ vs. $EP300^{\Delta/\Delta}$ iTreg cells, 22.08 ± 2.473 % vs. 14.32 ± 0.617%; Fig. 4L, M). Thus, these results indicate that EP300 deletion decreased the Treg cell population in allergic asthma. Furthermore, EP300 deficiency also impaired Treg cell functions.

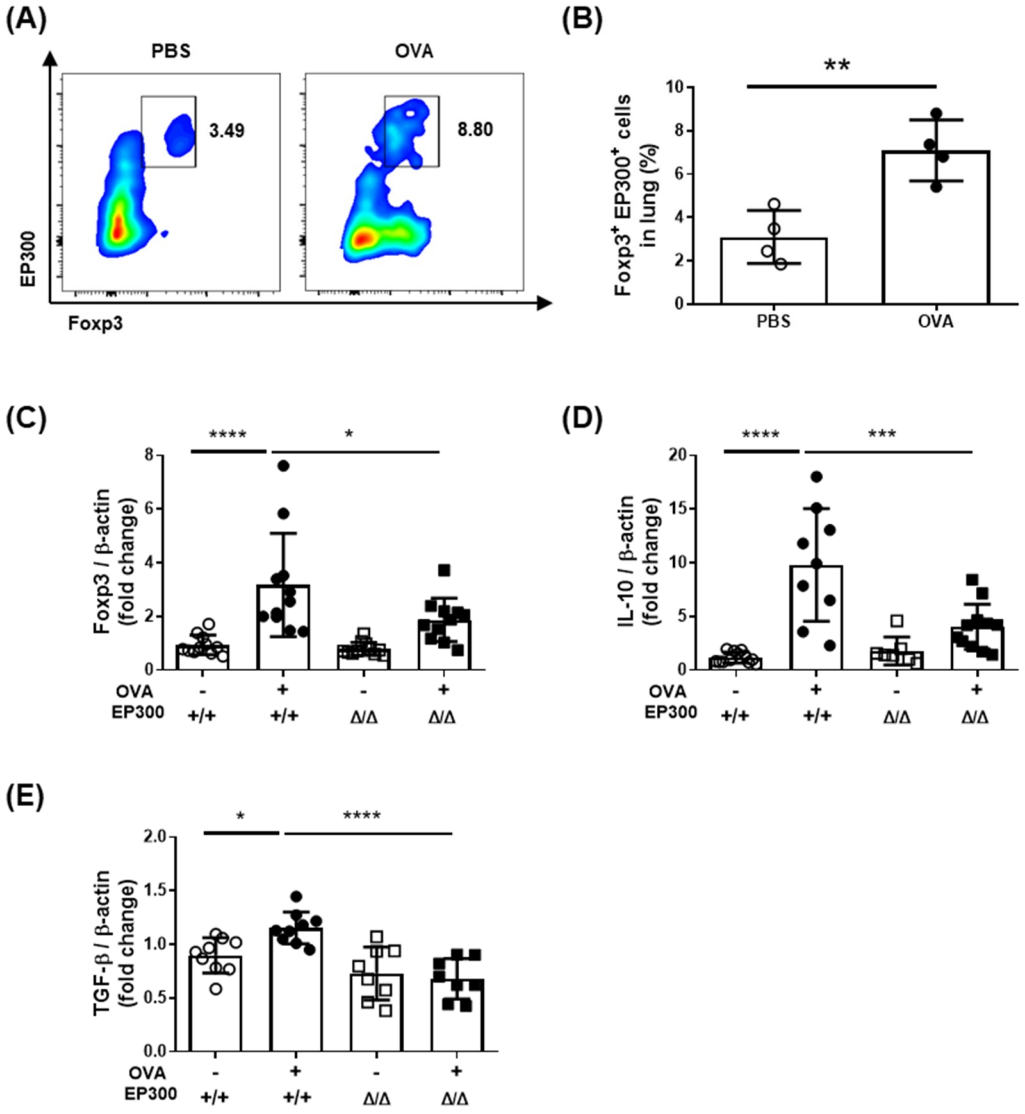

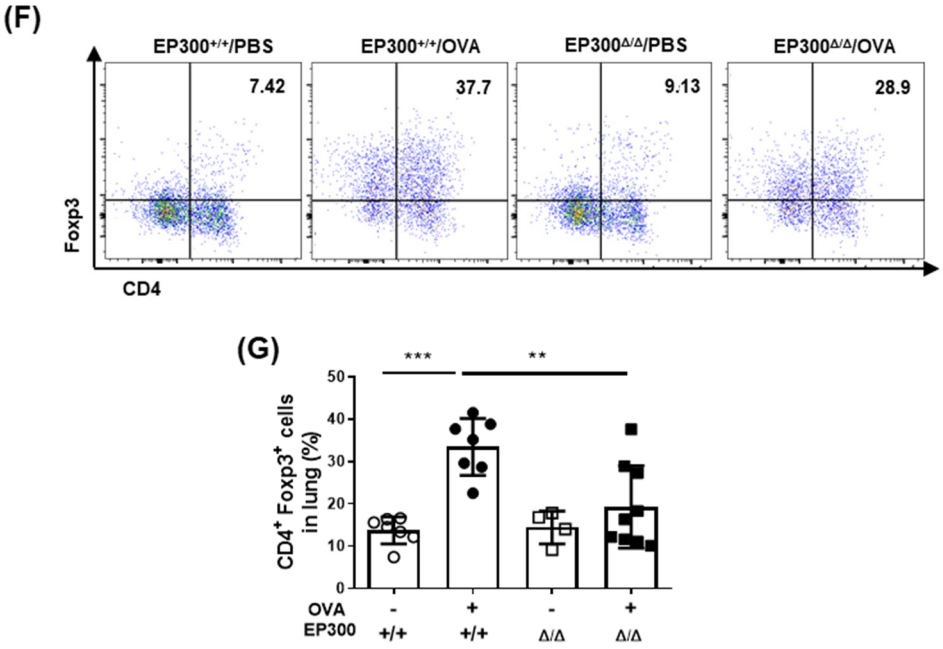

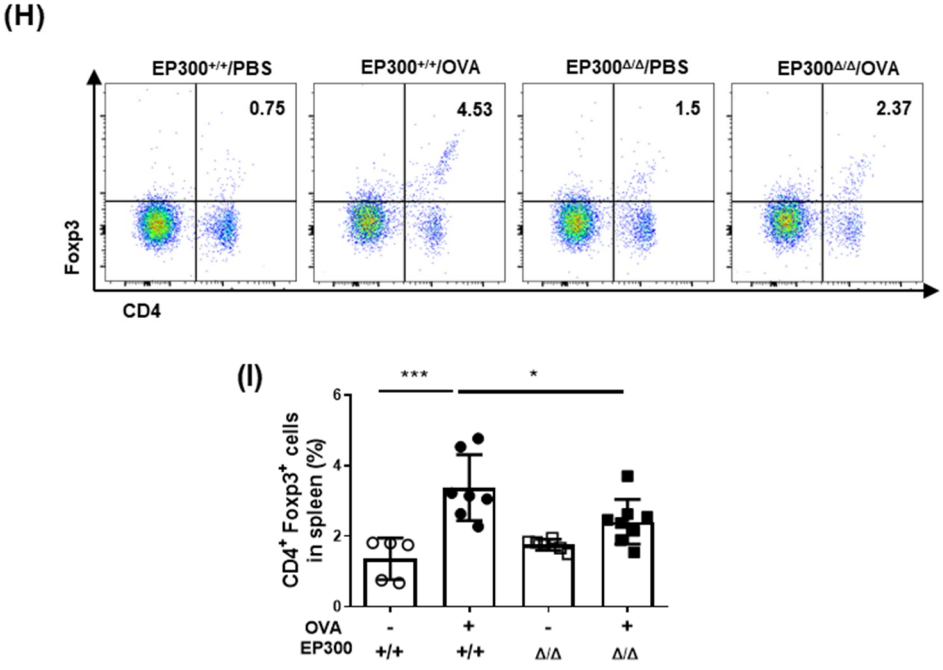

(J)

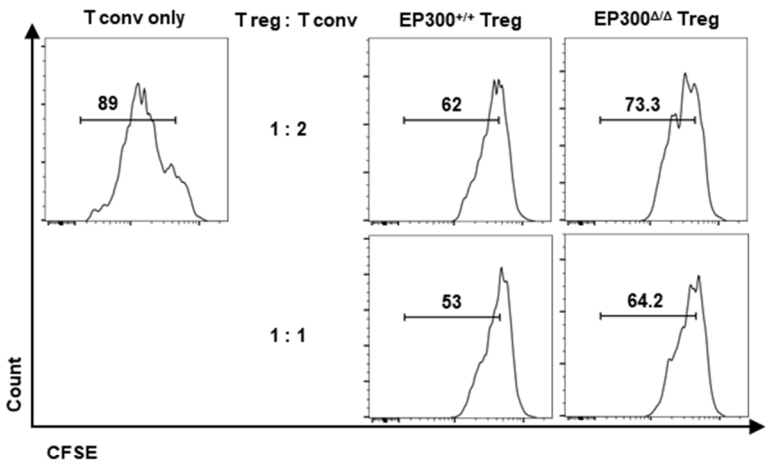

(K)

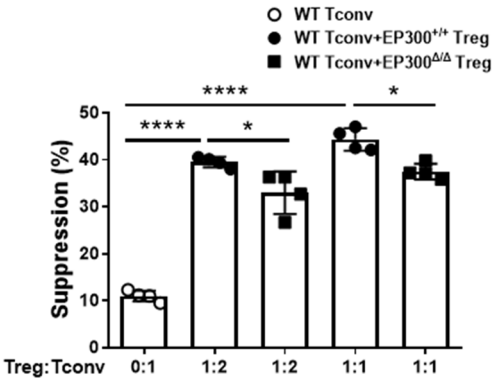

(L)

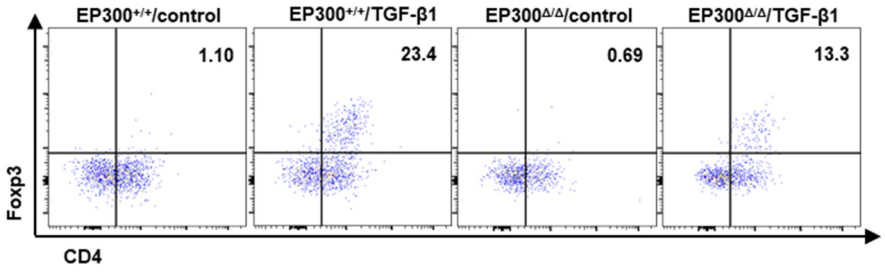

(M)

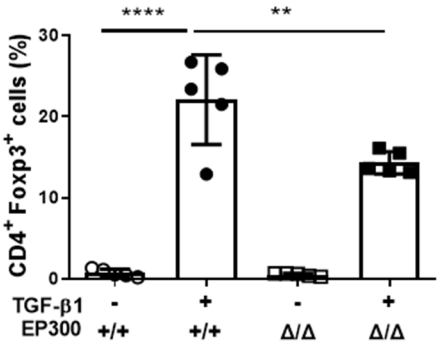

Fig. 4. EP300 deficiency reduces the population, suppression capacity, and differentiation potential of Treg cells. (A) Expression of EP300 in Treg cells in the lungs of $Foxp3^{DTR\text{-}GFP}$ mice was quantified by flow cytometry. (B) The graph represents the percentage of $Foxp3^{+}$ $EP300^{+}$ cells. (C-E) mRNA expression levels of Foxp3 (C), IL-10 (D), and TGF-β (E) in the lungs were measured by quantitative real-time PCR. (F-I) The frequency of Treg cells from the lungs (F) and spleen (H) was quantified by flow cytometry. The graph represents the percentage of $CD4^{+}$ $Foxp3^{+}$ cells in the lungs (G) and spleen (I). (J, K) Suppression assay using $CD4^{+}$ $CD25^{+}$ Treg cells sorted from the spleen of $EP300^{+/+}$ and $EP300^{\Delta/\Delta}$ mice. Flow cytometry analysis showed the population of proliferating Tconv cells (J), and the suppression percentage was determined by comparing the percentage of proliferating Tconv cells cultured alone to the percentage of proliferating Tconv cells in co-culture with $EP300^{+/+}$ or $EP300^{\Delta/\Delta}$ Treg cells at a ratio of 1:2 or 1:1 (Treg: Tconv) (K). (L, M) Differentiation assay using $CD4^{+}$ $CD25^{-}$ T cells isolated from the spleen of $EP300^{+/+}$ and $EP300^{\Delta/\Delta}$ mice. Flow cytometry analysis showed the population of cells differentiating into iTreg cells (L), and the graph represents the percentage of $CD4^{+}$ $Foxp3^{+}$ cells (M). The data are presented as the means ± SEM. *p*-values were analyzed by one-way ANOVA with Tukey's multiple comparisons. $^{*}p < 0.05$; $^{**}p < 0.01$; $^{***}p < 0.001$; $^{****}p < 0.0001$.

3.4. EP300 protects allergic asthma in a Treg cell-dependent manner

Given that EP300 could play a key role in Treg cell response, the Treg cell-specific role of EP300 in asthma was assessed. $EP300^{fl/fl}$ mice were crossed with $Foxp3^{eGFP\text{-}Cre\text{-}ERT2}$ mice to generate mice with inducible Foxp3-specific EP300 deletion, $EP300^{fl/fl}$;$Foxp3^{eGFP\text{-}Cre\text{-}ERT2}$ (hereafter, referred to as Foxp3-$EP300^{\Delta/\Delta}$) mice. $Foxp3^{eGFP\text{-}Cre\text{-}ERT2}$ (hereafter, referred to as Foxp3-$EP300^{+/+}$) mice were used as control animals. Afterward, depletion of EP300 was verified in $CD4^+$ $Foxp3^+$ Treg cells from the lungs, spleen, and dLNs of Foxp3-$EP300^{\Delta/\Delta}$ mice after tamoxifen treatment (Fig. 5A-F). Additionally, CBC analysis showed that the lymphocyte amount in Foxp3-$EP300^{+/+}$ and Foxp3-$EP300^{\Delta/\Delta}$ mice was in the normal range and did not significantly differ between the two groups (Table 3). Upon OVA treatment, airway resistance, airway eosinophilia, OVA-specific IgE, Th2 cytokine expression, and histological lung injury were increased in Foxp3-$EP300^{\Delta/\Delta}$ mice compared to Foxp3-$EP300^{+/+}$ mice (Fig. 5G-N). However, Treg cell populations were diminished in OVA-treated Foxp3-$EP300^{\Delta/\Delta}$ mice compared to those in OVA-treated Foxp3-$EP300^{+/+}$ mice (Fig. 5O, P). Collectively, these data suggest that Treg cell-specific EP300 ablation resulted in dysregulated type 2 immune responses and exacerbated airway inflammation.

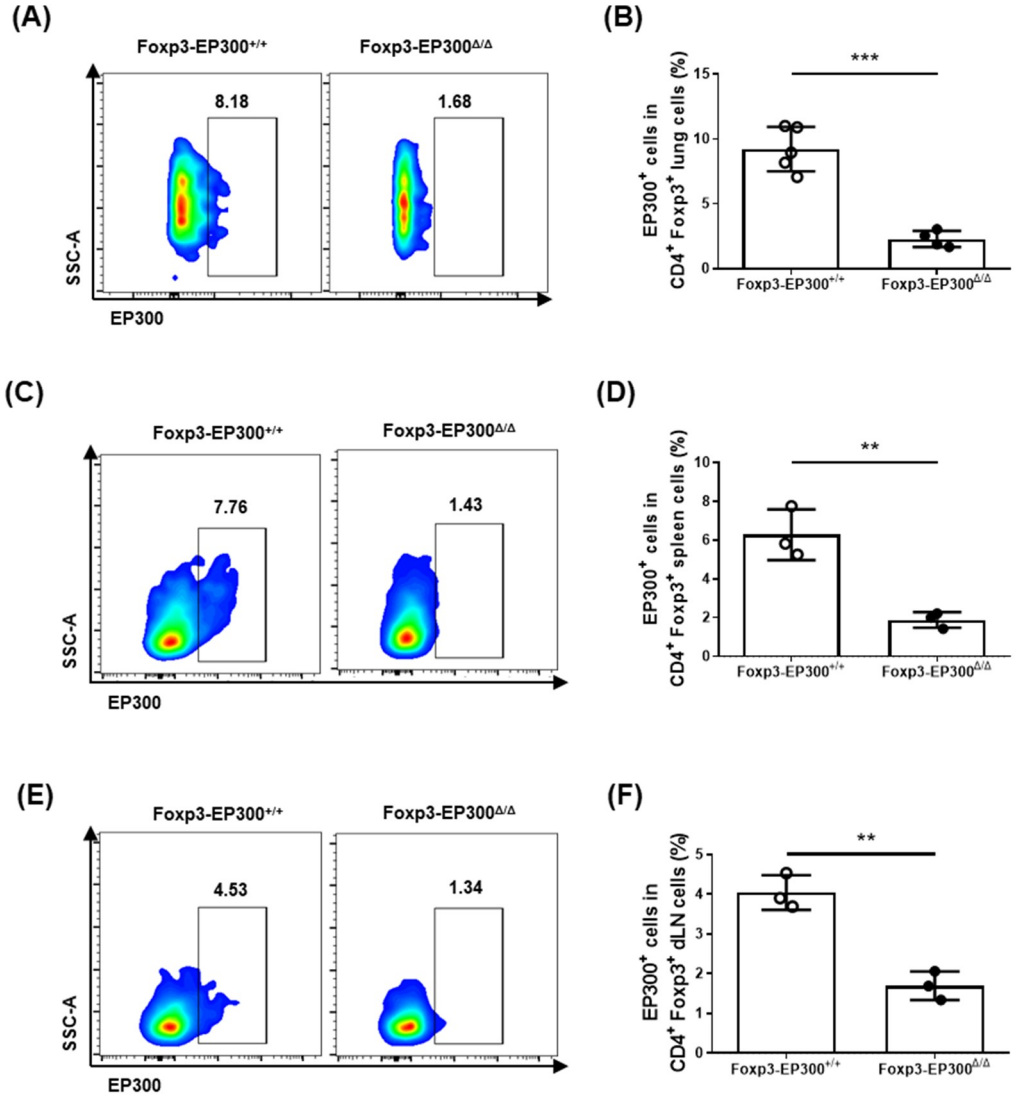

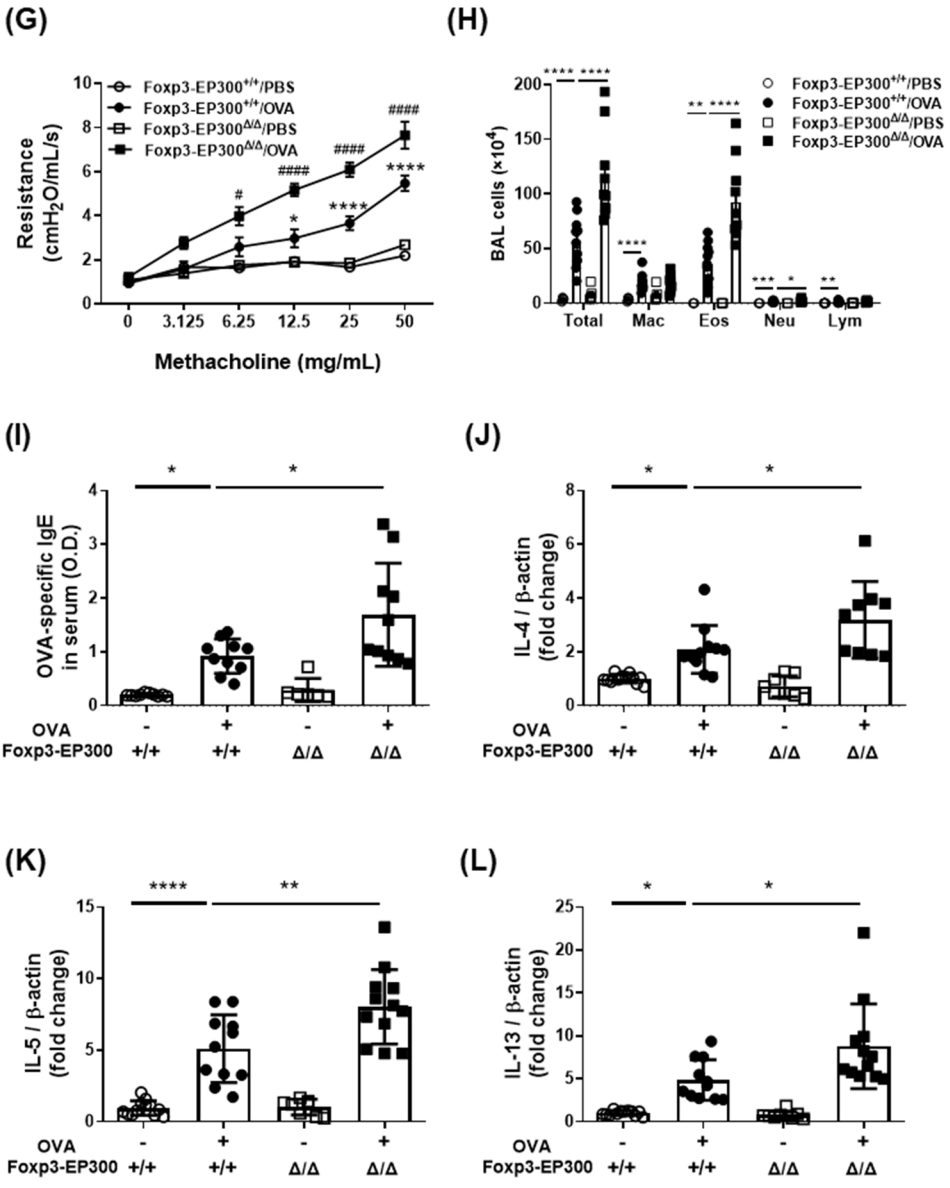

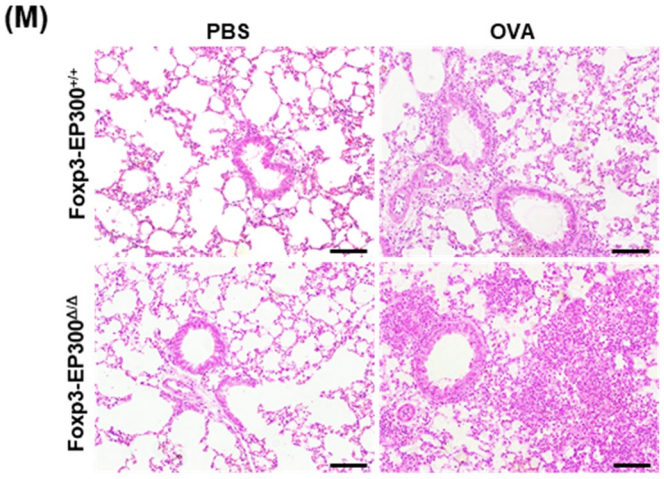

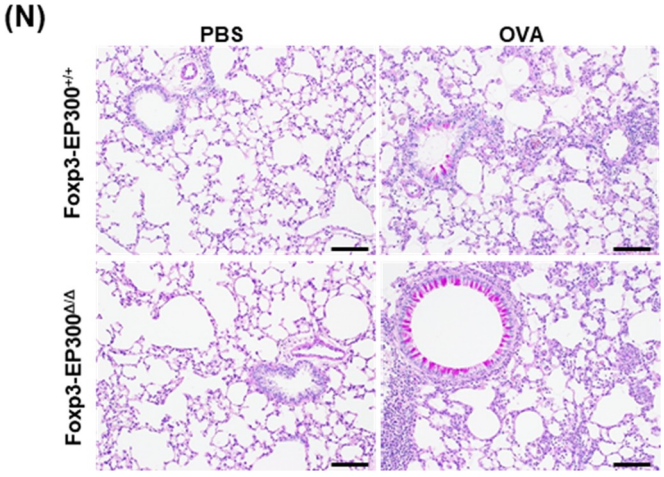

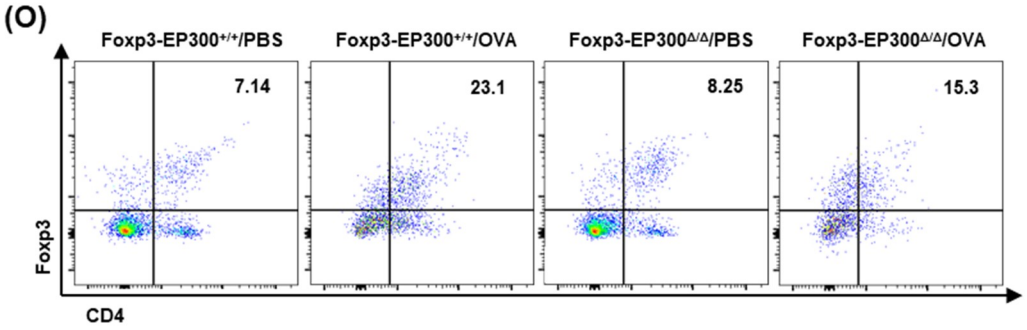

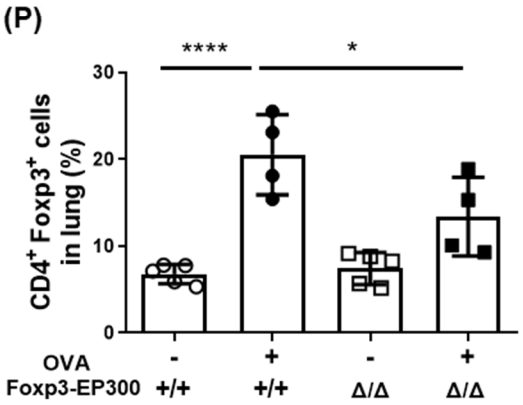

Fig. 5. Conditional deletion of EP300 in Foxp3-specific Treg cells aggravates type 2 inflammation. (A-F) Expression of EP300 in Treg cells from the lungs (A), spleen (C), and dLNs (E) of Foxp3-EP300$^{+/+}$ and Foxp3-EP300$^{\Delta/\Delta}$ mice was detected by flow cytometry. Each graph represents the proportion of EP300^{+} cells in CD4^{+} Foxp3^{+} cells derived from the lungs (B), spleen (D), and dLNs (F). (G) Airway resistance in response to methacholine was assessed using the FlexiVent system. (H) Inflammatory cells in BALF were counted. (I) OVA-specific IgE levels in the serum were assessed by ELISA. (J-L) mRNA expression levels of IL-4 (J), IL-5 (K), and IL-13 (L) in the lungs were measured by quantitative real-time PCR. (M, N) Inflammatory cell infiltration and mucus production in the lungs were determined by H&E staining (M) and PAS staining (N), respectively. The scale bar indicates 100 μm. (O, P) The population of Treg cells from the lungs was quantified by flow cytometry (O), and the graph represents the percentage of CD4^{+} Foxp3^{+} cells in the lungs (P). The data are presented as the means ± SEM. *p*-values were analyzed by one-way ANOVA with Tukey's multiple comparisons tests. $^{*}p < 0.05$; $^{**}p < 0.01$; $^{***}p < 0.001$; $^{****}p < 0.0001$. In figure (G) $^{*}p < 0.05$, $^{****}p < 0.0001$ for Foxp3-EP300$^{+/+}$/PBS vs. Foxp3-EP300$^{+/+}$/OVA and $^{\#}p < 0.05$, $^{\#\#\#\#}p < 0.0001$ for Foxp3-EP300$^{+/+}$/OVA vs. Foxp3-EP300$^{\Delta/\Delta}$/OVA.

Table 3. CBC analysis of Foxp3-EP300$^{+/+}$ and Foxp3-EP300$^{\Delta/\Delta}$ mice

Blood count parameters	Foxp3-EP300$^{+/+}$ (n = 3)	Foxp3-EP300$^{\Delta/\Delta}$ (n = 3)	Normal range
White blood cells, 10^3/μl	3.53 ± 0.54	2.70 ± 0.03	0.80-10.60
Neutrophils, %	11.90 ± 2.20	11.83 ± 2.52	6.5-50.0
Lymphocytes, %	84.20 ± 2.85	84.47 ± 2.06	40.0-92.0
Monocytes, %	1.77 ± 0.25	2.43 ± 0.42	0.9-18.0
Eosinophils, %	2.10 ± 0.70	1.27 ± 0.35	0.0-7.5
Basophils, %	0.03 ± 0.06	0.00 ± 0.00	0.0-1.5

3.5. Transcriptional activation of GBP5 by EP300 modulates Treg cells

To elucidate the molecular mechanisms of EP300 in Treg cells, ChIP-Seq and RNA-Seq were performed. Treg cells were sorted from the lungs of PBS or OVA-treated Foxp3-EP300$^{+/+}$ and Foxp3-EP300$^{\Delta/\Delta}$ mice. The purity of sorted Treg cells was >95% (Fig. 6A). ChIP-Seq showed that a total of 3,647 genes exhibited at least one EP300-binding peak in Treg cells from OVA-treated Foxp3-EP300$^{+/+}$ mice. These results were not observed with Treg cells of OVA-treated Foxp3-EP300$^{\Delta/\Delta}$ mice. RNA-Seq data revealed that the expression of 1,603 genes was significantly increased in the Treg cells of OVA-treated Foxp3-EP300$^{+/+}$ mice than in PBS-treated Foxp3-EP300$^{+/+}$ mice. Of these, 273 and 159 genes were upregulated and downregulated, respectively, in Treg cells of OVA-treated Foxp3-EP300$^{\Delta/\Delta}$ mice than those in OVA-treated Foxp3-EP300$^{+/+}$ mice. Of the 273 upregulated genes, 30 genes overlapped with ChIP-Seq data, and 20 genes out of the 159 downregulated genes overlapped with ChIP-Seq data (Fig. 6B). The heatmap showed overlapping patterns of differentially expressed genes (DEGs) in Treg cells of Foxp3-EP300$^{+/+}$ and Foxp3-EP300$^{\Delta/\Delta}$ mice (Fig. 6C). Furthermore, pathway enrichment analysis was performed based on those genes using the GO database. The results and revealed that the top ten pathways were primarily associated with inflammatory response and chemotaxis (Fig. 6D). Statistically significant genes in the top ten GO pathway categories are summarized in Table 4.

To identify the primary target gene of EP300 in Treg cells during asthma induction, a dataset of 3,647 ChIP-Seq-identified genes and 159 downregulated RNA-Seq genes with previously established datasets of Foxp3 target genes. In previous studies, TJ Sadlon et al.[28] showed a set of 5,580 Foxp3 target genes in human Treg cells. Furthermore, data from Foxp3 ChIP-Atlas (http://chip-atlas.org) have demonstrated a set of 1,000 genes. Upon combining all four datasets separately, the *GBP5* gene overlapped across all groups (Fig. 6E). To further elucidate the interaction of EP300 with GBP5, the processed ChIP-Seq data were visualized using IGV software. Prominent peaks of H3K9ac and EP300 were noted in correspondence with the *GBP5* gene in the Treg cells of OVA-treated Foxp3-EP300$^{+/+}$ mice, which were weak or absent in Treg cells of OVA-treated Foxp3-EP300 $^{\Delta/\Delta}$ mice (Fig. 6F). Additionally, three putative EP300 binding sites were found in the transcription regions of *GBP5* in OVA-treated Foxp3-EP300$^{+/+}$ Treg cells, which are summarized in Table 5. Next, transcriptional expression of GBP5 was

also validated by real-time PCR in sorted lung Treg cells. GBP5 expression in Treg cells was significantly elevated in OVA-treated Foxp3-EP300$^{+/+}$ mice than in PBS-treated Foxp3-EP300$^{+/+}$ mice but was reduced in OVA-treated Foxp3-EP300$^{\Delta/\Delta}$ mice (Fig. 6G). Since *GBP5* was discovered as a primary target gene of EP300 in Treg cells, GBP5 knockdown studies were performed to confirm whether GBP5 modulates the Treg cell responses such as proliferation. GBP5 expression was increased by CD3/28 stimulation in iTreg cells transfected with si-control, whereas GBP5 expression was remarkably suppressed in iTreg cells transfected with si-GBP5 (Fig. 6H). Next, iTreg cell proliferation was significantly reduced in CD3/28-stimulated si-GBP5 cells than that in CD3/28-stimulated si-control cells (Fig. 6I). Subsequently, it was investigated whether EP300 mediated the activation of GBP5 in proliferating Treg cells. As shown in Fig. 6J, the augmented proliferation of iTreg cells after CD3/28 stimulation was significantly reduced by C646 treatment, an EP300 inhibitor. Furthermore, GBP5 expression in iTreg cells was markedly decreased by C646 treatment upon CD3/28 stimulation (Fig. 6K). Since EP300 mediates the proliferation of Treg cells and transcriptional activation of GBP5, we next examined whether EP300 enhances Treg cell responses via GBP5. To do this, we investigated the effect of GBP5 overexpression on the reduction in Treg cell proliferation caused by EP300 depletion. Treg cells transduced with control vector LV (LV-control) or GBP5 overexpression vector LV (LV-GBP5) were identified based on mCherry expression by fluorescence microscopy (Fig. 6L). Subsequently, Treg cell proliferation was attenuated in LV-control cells of Foxp3-EP300$^{\Delta/\Delta}$ mice than in the LV-control cells of Foxp3-EP300$^{+/+}$ mice after CD3/28 stimulation. However, LV-GBP5 cells of Foxp3-EP300$^{\Delta/\Delta}$ mice restored the Treg cell proliferation, similar to the LV-control cells of Foxp3-EP300$^{+/+}$ mice upon CD3/28 stimulation (Fig. 6M). Hence, overexpression of GBP5 restored the reduced Treg cell proliferation by depletion of EP300, indicating the functional significance of GBP5 in Treg cells.

Collectively, it was demonstrated that GBP5, a target gene of EP300, can control the Treg cell response in an EP300-dependent manner, and EP300-specific Treg cell responses can modulate Th2 inflammation in allergic asthma (Figure 7).

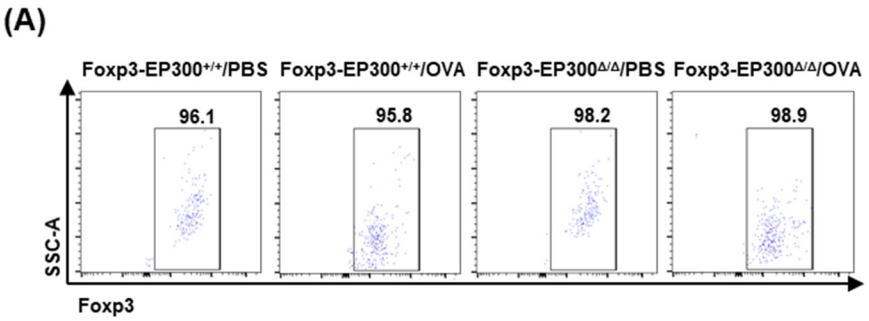

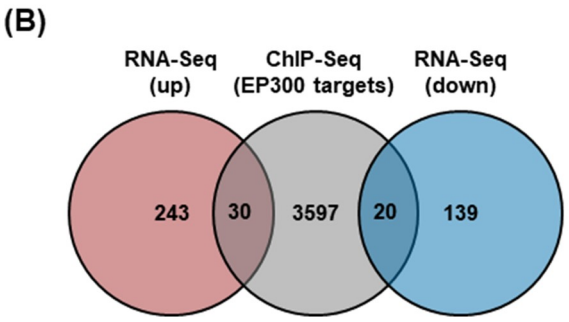

(C)

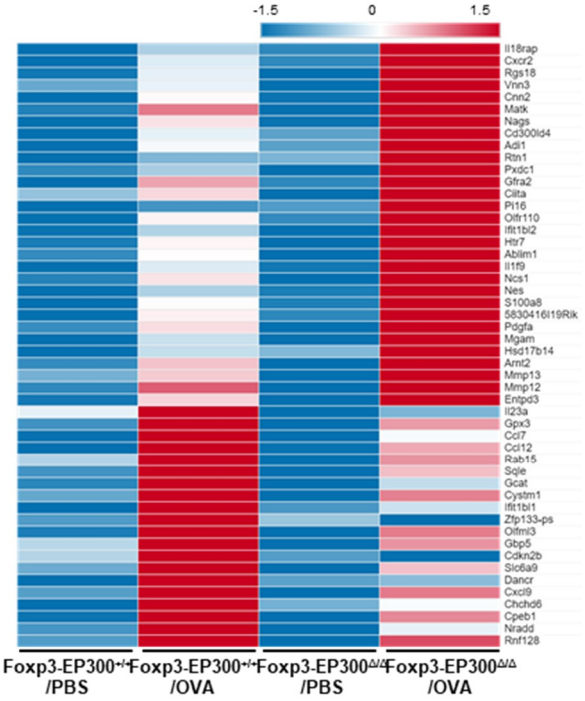

(D)

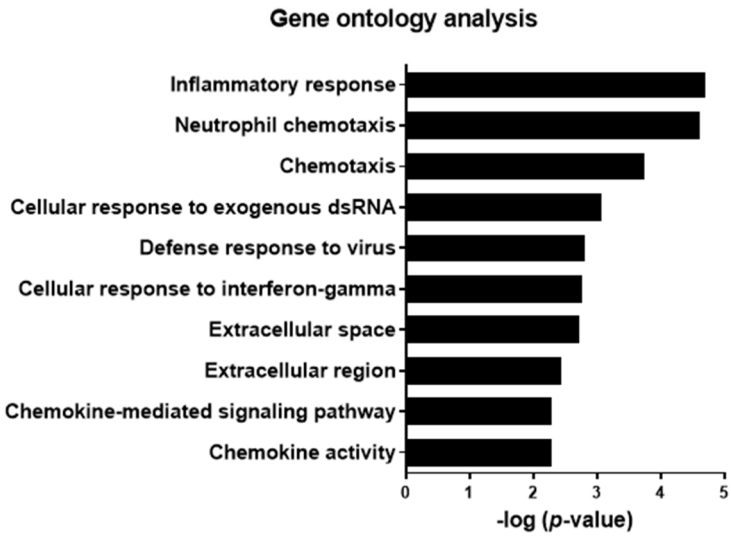

(E)

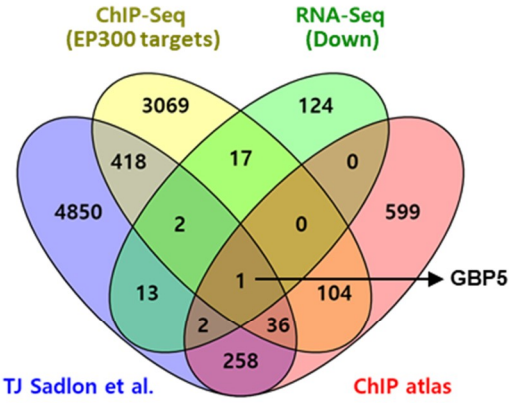

(F)

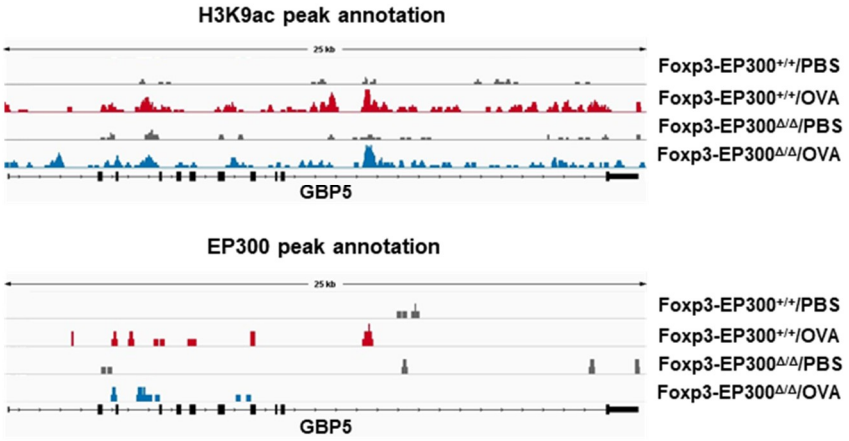

(G)

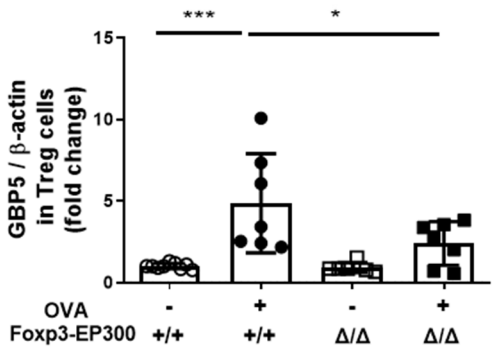

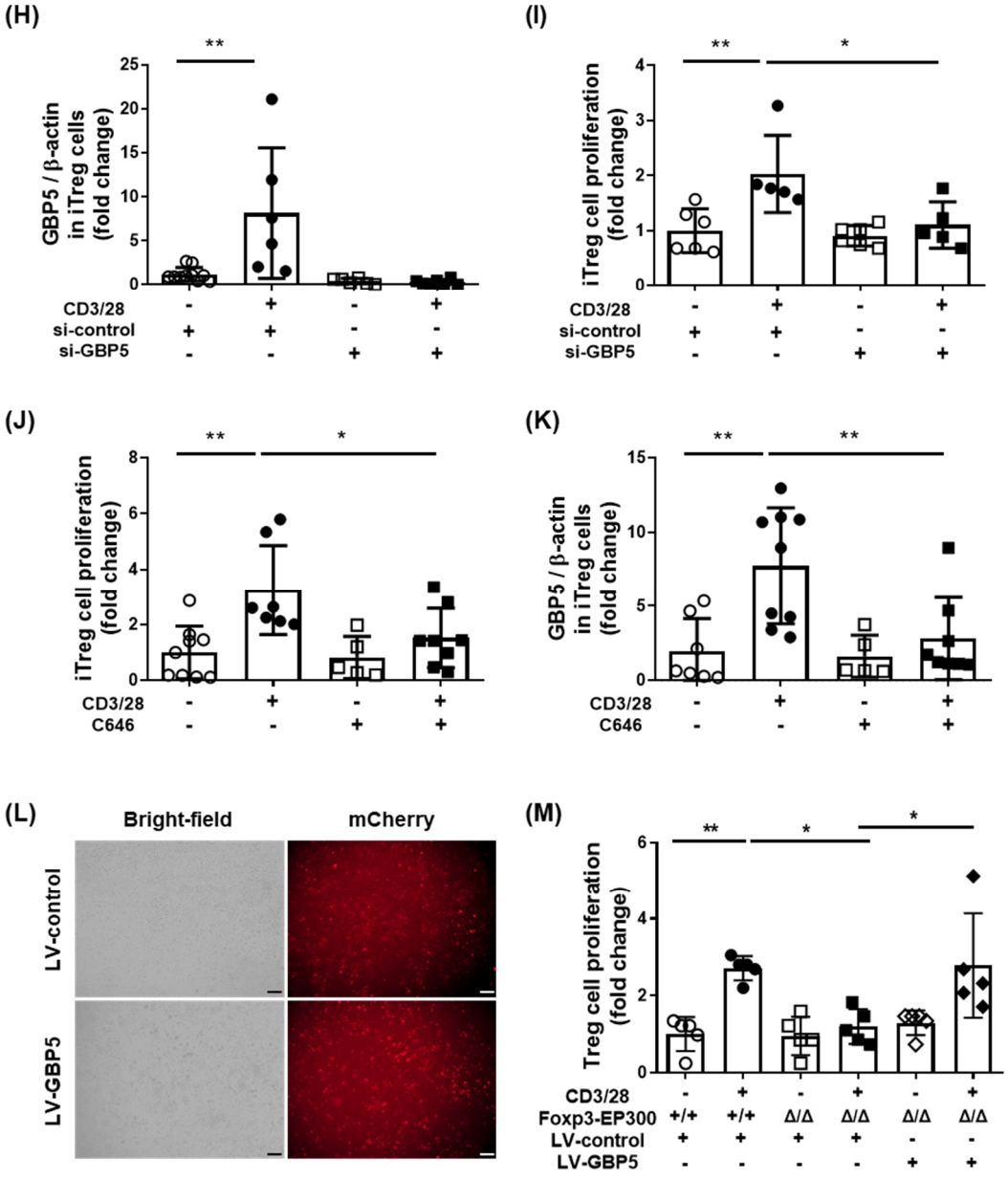

Fig. 6. Integration of ChIP-Seq and RNA-Seq identified *GBP5* as a target gene of EP300 in Treg cells. (A) Fluorescence-activated cell sorting plots show the gating strategy for sorted $CD4^+$ $Foxp3^+$ Treg cells derived from the lungs of Foxp3-$EP300^{+/+}$ and Foxp3-$EP300^{\Delta/\Delta}$ mice. (B) Venn diagram shows the gene number in EP300-bound genes identified by ChIP-Seq and DEGs identified by RNA-Seq. (C) The heat map indicates the overlapping DEGs identified by combining ChIP-Seq and RNA-Seq. (D) The graph represents the top 10 GO terms ordered by -log10 of *p*-value after GO enrichment analysis. (E) Four ellipse Venn diagram shows the gene number comparing data derived from ChIP-Seq and RNA-Seq with Foxp3 target gene data depicted from previous Foxp3 ChIP-Seq study and Foxp3 ChIP-Atlas database. (F) H3K9ac (top) and EP300 (bottom) peaks were visualized in the transcriptional regions associated with *GBP5* by IGV. (G) GBP5 mRNA expression in the Treg cells in the lungs was measured by quantitative real-time PCR. (H, I) GBP5 expression in transfected iTreg cells was confirmed by quantitative real-time PCR (H), and the proliferation of transfected iTreg cells was determined by the CCK-8 assay (I). (J, K) The proliferation of inhibitor-treated iTreg cells was assessed using the CCK-8 assay (J), and GBP5 expression in inhibitor-treated iTreg cells was measured by quantitative real-time PCR (K). (L) Bright-field and mCherry fluorescence images show control or GBP5 LV-transduced Treg cells on day two after transduction. The scale bar indicates 100 μm. (M) The proliferation of LV-transduced Treg cells was determined by the CCK-8 assay. The data are presented as the means ± SEM. *p*-values were analyzed by one-way ANOVA with Tukey's multiple comparisons tests. $^{*}p < 0.05$; $^{**}p < 0.01$; $^{***}p < 0.001$.

Table 4. Detailed analysis of top 10 gene ontology (GO) pathways

GO ID	Term	Genes
GO:0006954	Inflammatory response	*S100A8, IL18RAP, GBP5, CXCL9, CCL12, CIITA, IL23A, CCL7*
GO:0030593	Neutrophil chemotaxis	*S100A8, CXCL9, CCL12, CCL7, CXCR2*
GO:0006935	Chemotaxis	*S100A8, CXCL9, CCL12, CCL7, CXCR2*
GO:0071360	Cellular response to exogenous dsRNA	*IFIT1BL1, CIITA, IFIT1BL2*
GO:0051607	Cellular response to interferon-gamma	*IFIT1BL1, GBP5, CXCL9, IL23A, IFIT1BL2*
GO:0071346	Extracellular space	*GBP5, CCL12, CIITA, CCL7*
GO:0005615	Extracellular region	*S100A8, PI16, VNN3, MMP13, CXCL9, CCL12, OLFML3, PDGFA, MMP12, IL23A, CCL7, GPX3*
GO:0005576	Defense response to virus	*S100A8, PI16, MMP13, CXCL9, CCL12, OLFML3, PDGFA, MMP12, IL23A, CCL7, GPX3*
GO:0070098	Chemokine-mediated signaling pathway	*CXCL9, CCL12, CCL7*
GO:0008009	Chemokine activity	*CXCL9, CCL12, CCL7*

GO, gene ontology.

Table 5. Predictive EP300 binding sites of *GBP5* based on ChIP-Seq

Gene		Start	End	Distance to TSS	Annotation
GBP5	#1	142490430	142490897	-6037	Distal intergenic
	#2	142493651	142494031	-2903	Promoter (2–3 kb)
	#3	142496543	142497788	0	Promoter (≤1 kb)

TSS, transcription start site.

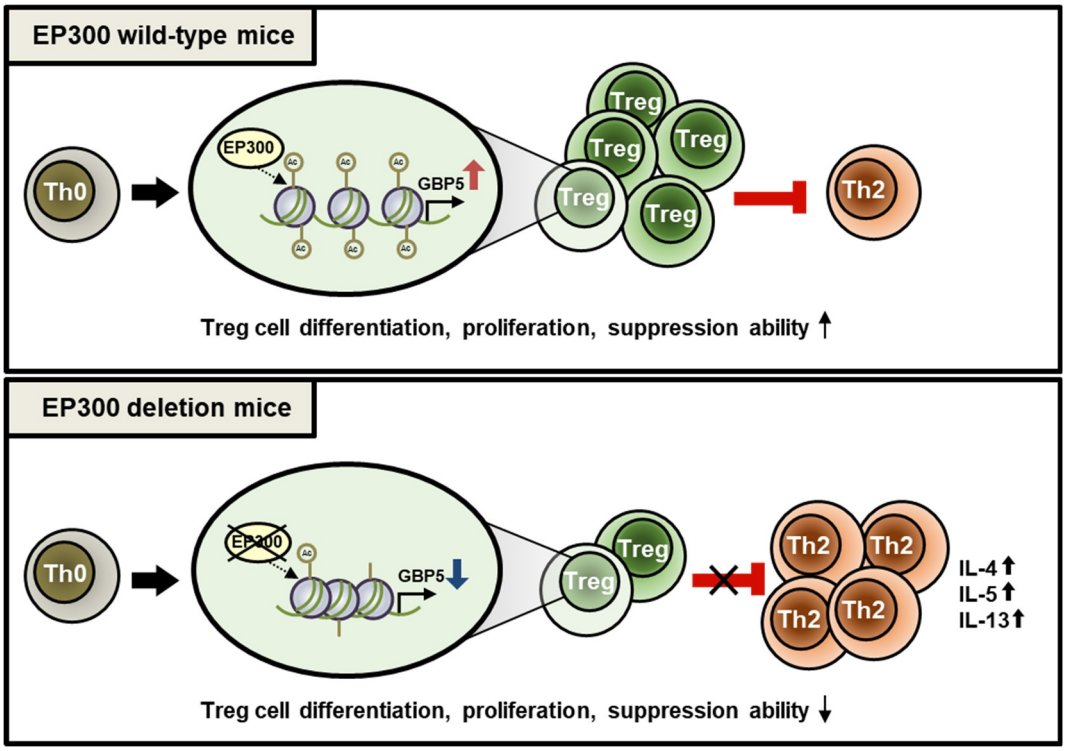

Fig. 7. EP300 participates in Th2 immune responses by regulating Treg cells through activation of GBP5. In wild-type mice, differentiation from naïve T cells to Treg cells is normally induced, and EP300 promotes Treg cell proliferation by increasing transcriptional activation of GBP5. However, in EP300 deletion mice, the differentiation potential of Treg cells is impaired, and transcriptional activation of GBP5 in Treg cells is reduced, resulting in weakened Treg cell proliferation. Consequently, Treg cells cannot effectively suppress the Th2 inflammation, and these responses may exacerbate asthma.

4. Discussion

This study elucidated a novel role for EP300 in the pathogenesis of allergic asthma. Increased expression of EP300 in Treg cells led to transcriptional activation of GBP5, thereby enhancing Treg cell proliferation. Enhanced Treg cell responses suppressed Th2 inflammation and airway hyperresponsiveness in asthma.

Epigenetic dysregulation is associated with the pathogenesis of chronic inflammatory disease, particularly asthma, via environmental effects including exposure to cigarette smoke, air pollutants, and chemical substances.[29] Histone acetylation, a critical epigenetic modification, modifies the accessibility of genomic DNA by creating more open and transcriptionally active chromatin and allows transcription factors and RNA polymerase to initiate gene transcription. HAT enzymes, such as EP300, catalyze the reaction.[30,31] EP300 modulates fundamental biological processes such as cell growth, development, and apoptosis.[14,32] Compared to healthy controls, increased HAT levels were observed in bronchial biopsy and BALF samples derived from patients with asthma.[33,34] Consistently, in this study, we found that HAT activity was augmented in OVA or HDM-treated mice, and the expression of EP300 was significantly increased in asthma-induced mice and patients with asthma. EP300 expression is increased in various immune cells upon asthma induction because EP300 is a histone acetyltransferase. Especially, EP300 can be expressed in the immune tolerance cells such as Treg cells, which play a protective role in asthma, and can induce anti-inflammatory cytokines such as TGF-β and IL-10. Therefore, increased EP300 expression might be involved in a protective role in the immune response to allergens. Altogether, these results highlight that EP300 is associated with allergic asthma, contributing to the release of inflammatory mediators and representing molecular mechanisms of airway inflammation.

An imbalance between Th2 cells and Treg cells in type 2 immune response plays a central role in the immunopathology of allergic diseases.[35] Treg cells are major negative regulatory cells involved in the immune response that suppress Th2 responses to allergens. Furthermore, they mediate the development of tolerogenic dendritic cells and regulatory B cells.[36] Thus, regulation of the Th2/Treg cell balance via main transcription factors STAT6, GATA3, and Foxp3 presents a potential therapeutic strategy for controlling allergic asthma.[37] Previous studies showed increased histone acetylation at specific Th2 and Treg cell-related loci in $CD4^+$

T cells from allergic asthma patients compared to healthy controls.[38,39] Furthermore, conditional deletion or pharmacological inhibition of EP300 in Treg cells increases apoptosis and impairs Treg cell suppressive function and peripheral Treg cell induction, thereby confirming the importance of EP300 in Treg cell functions and homeostasis.[19] Consistent with previous results, this study showed that systemic or Treg cell-specific loss of EP300 increased disease severity, including airway inflammation, by elevating Th2 immune responses and decreasing the Treg cell population. Moreover, it was confirmed that EP300 controlled the suppressive capacity and differentiation potential of Treg cells. Based on these findings, this study unraveled the physiological roles of EP300 in asthma and provided evidence that EP300 is pivotal for controlling airway inflammation by regulating the function of Treg cells. However, further studies will be required to identify additional epigenetic mechanisms involved in the regulation of Treg cells in addition to EP300-mediated acetylation.

Foxp3 transcription factor is a representative regulator of Treg cell formation and function maintenance, whose activity is influenced by diverse epigenetic mechanisms.[40] Based on the target genes of EP300 identified through ChIP-Seq and RNA-Seq together with the target genes of Foxp3 identified through previous studies, *GBP5* was confirmed as an important target gene of EP300 in Treg cells during asthma induction. GBP5 is a member of the TRAFAC class dynamin-like GTPase superfamily that plays a central role in cell-intrinsic immunity.[41] Furthermore, GBP5 is involved in a variety of diseases, including cancer. In a previous study, GBP5 overexpression enhanced the proliferation, migration, and invasion of glioblastoma cells via the activation of the Src/ERK1/2/MMP3 axis, but silencing GBP5 had a contrasting effect.[42] Moreover, GBP5 regulated the cell cycle and cancer stemness in oral squamous cell carcinoma cells. GBP5 knockdown reduced cell growth and arrested it in the G1 phase.[41] Single-cell analysis of colorectal cancer indicated that *GBP5* was primarily expressed in myeloid cells and T cells, and *GBP5* expression in T cells was similar to that of Treg cell markers Foxp3 and IL2Ra.[43] The *GBP5* gene was differentially expressed in human Treg cells compared to naïve T cells, and a recent transcriptomic study performed on patients with asthma indicated that the expression of *GBP5* was increased in allergen-reactive Treg cells.[44,45] In this study, the knockdown of GBP5 decreased Treg cell proliferation and treatment with an EP300 inhibitor suppressed GBP5 expression in Treg cells. Moreover, reduced Treg cell proliferation in EP300-deficient Treg cells was restored upon GBP5 overexpression. These results suggest that GBP5

may play an essential role in Treg cells during asthma development. Furthermore, EP300 can mediate the transcriptional activation of GBP5, leading to the modulation of Treg cells. However, additional research will be needed to determine the detailed mechanism by which GBP5 regulates Treg cells. Additionally, the previous study of pulmonary fibrosis has shown that EP300 mediated transcriptional activation of the chemokines CCL2, CCL7, and CCL12 in type 2 alveolar cells, consequently promoting pulmonary fibrosis.[46] In this study, ChIP-Seq and RNA-Seq analysis with Treg cells upon asthma induction also revealed that EP300 modulated various chemokine-related genes, such as *S100A8*, *CXCL9*, *CCL12*, *CCL7*, and *CXCR2*. These genes are associated with the regulation of Treg cell migration, recruitment, and differentiation.[47-49] Therefore, the chemokine-mediated immune responses of Treg cells can be partially involved in the immunological regulation of EP300 in allergic asthma.

5. Conclusion

Overall, this study suggests that EP300 plays a central role in Th2/Treg cell balance in the pathogenesis of allergic asthma. Initially, the expression of EP300 was elevated in asthma mouse models and asthma patients. Next, type 2 airway inflammation was increased and the Treg cell population was reduced in systemic EP300 deletion mice compared to control mice. Additionally, EP300 deletion decreased the suppression ability and differentiation potential of Treg cells. Treg cell-specific EP300 deletion mice also had deteriorated airway hyperresponsiveness and allergic inflammation compared with control mice. Lastly, *GBP5* was identified as a main EP300 target gene, and it was verified that EP300 regulates Treg cell proliferation by GBP5 modulation. These results highlight that EP300 exerted a protective effect during the pathogenesis of allergic asthma. EP300 can be used as a biomarker of asthma, and the activators or enhancers of EP300 could provide new therapeutic options. Therapies that focus on enhancing Treg cell function, possibly via EP300 modulation, could be developed to control asthma more effectively. Further research will be needed on EP300 levels and correlation with disease severity. Furthermore, long-term studies involving patients with asthma are necessary to validate EP300 as a reliable biomarker and understand its role in disease progression and response to treatment. Taken together, our findings suggest the significance of EP300 in asthma and the possibility of the development of a new approach to the diagnosis, management, and treatment of asthma.

References

1. Papi A, Brightling C, Pedersen SE, Reddel HK. Asthma. Lancet 2018;391:783-800.
2. Fahy JV. Type 2 inflammation in asthma--present in most, absent in many. Nat Rev Immunol 2015;15:57-65.
3. Lloyd CM, Hessel EM. Functions of T cells in asthma: more than just T(H)2 cells. Nat Rev Immunol 2010;10:838-48.
4. Porsbjerg C, Melén E, Lehtimäki L, Shaw D. Asthma. Lancet 2023;401:858-73.
5. Cao TBT, Quoc QL, Jang JH, Park HS. Immune Cell-Mediated Autoimmune Responses in Severe Asthma. Yonsei Med J 2024;65:194-201.
6. Sharma S, Yang IV, Schwartz DA. Epigenetic regulation of immune function in asthma. J Allergy Clin Immunol 2022;150:259-65.
7. Yang IV, Schwartz DA. Epigenetic mechanisms and the development of asthma. Journal of Allergy and Clinical Immunology 2012;130:1243-55.
8. Hammad H, Lambrecht BN. The basic immunology of asthma. Cell 2021;184:1469-85.
9. Hori S, Nomura T, Sakaguchi S. Control of regulatory T cell development by the transcription factor Foxp3. Science 2003;299:1057-61.
10. Shevach EM, Davidson TS, Huter EN, Dipaolo RA, Andersson J. Role of TGF-Beta in the induction of Foxp3 expression and T regulatory cell function. J Clin Immunol 2008;28:640-6.
11. Khan MA. Regulatory T cells mediated immunomodulation during asthma: a therapeutic standpoint. J Transl Med 2020;18:456.
12. Fontenot JD, Gavin MA, Rudensky AY. Foxp3 programs the development and function of CD4+CD25+ regulatory T cells. Nat Immunol 2003;4:330-6.
13. Brook PO, Perry MM, Adcock IM, Durham AL. Epigenome-modifying tools in asthma. Epigenomics 2015;7:1017-32.
14. Potaczek DP, Harb H, Michel S, Alhamwe BA, Renz H, Tost J. Epigenetics and allergy: from basic mechanisms to clinical applications. Epigenomics 2017;9:539-71.
15. Kabesch M, Adcock IM. Epigenetics in asthma and COPD. Biochimie 2012;94:2231-41.
16. Ntontsi P, Photiades A, Zervas E, Xanthou G, Samitas K. Genetics and Epigenetics in Asthma. Int J Mol Sci 2021;22.

17. Ogryzko VV, Schiltz RL, Russanova V, Howard BH, Nakatani Y. The transcriptional coactivators p300 and CBP are histone acetyltransferases. Cell 1996;87:953-9.
18. Dancy BM, Cole PA. Protein lysine acetylation by p300/CBP. Chem Rev 2015;115:2419-52.
19. Liu Y, Wang L, Predina J, Han R, Beier UH, Wang LC, et al. Inhibition of p300 impairs Foxp3^{+} T regulatory cell function and promotes antitumor immunity. Nat Med 2013;19:1173-7.
20. Valor LM, Viosca J, Lopez-Atalaya JP, Barco A. Lysine acetyltransferases CBP and p300 as therapeutic targets in cognitive and neurodegenerative disorders. Curr Pharm Des 2013;19:5051-64.
21. Barnes PJ, Adcock IM, Ito K. Histone acetylation and deacetylation: importance in inflammatory lung diseases. European Respiratory Journal 2005;25:552-63.
22. Wang Y, Zhou C, Gao H, Li C, Li D, Liu P, et al. Therapeutic effect of Cryptotanshinone on experimental rheumatoid arthritis through downregulating p300 mediated-STAT3 acetylation. Biochem Pharmacol 2017;138:119-29.
23. Cui ZL, Gu W, Ding T, Peng XH, Chen X, Luan CY, et al. Histone modifications of Notch1 promoter affect lung CD4+ T cell differentiation in asthmatic rats. Int J Immunopathol Pharmacol 2013;26:371-81.
24. van Loosdregt J, Vercoulen Y, Guichelaar T, Gent YY, Beekman JM, van Beekum O, et al. Regulation of Treg functionality by acetylation-mediated Foxp3 protein stabilization. Blood 2010;115:965-74.
25. Zhang Y, Liu T, Meyer CA, Eeckhoute J, Johnson DS, Bernstein BE, et al. Model-based analysis of ChIP-Seq (MACS). Genome Biol 2008;9:R137.
26. Yu CH, Dang Y, Zhou Z, Wu C, Zhao F, Sachs MS, et al. Codon Usage Influences the Local Rate of Translation Elongation to Regulate Co-translational Protein Folding. Mol Cell 2015;59:744-54.
27. Venuprasad K, Kong YC, Farrar MA. Control of Th2-mediated inflammation by regulatory T cells. Am J Pathol 2010;177:525-31.
28. Sadlon TJ, Wilkinson BG, Pederson S, Brown CY, Bresatz S, Gargett T, et al. Genome-wide identification of human FOXP3 target genes in natural regulatory T cells. J Immunol 2010;185:1071-81.

29. Sheikhpour M, Maleki M, Ebrahimi Vargoorani M, Amiri V. A review of epigenetic changes in asthma: methylation and acetylation. Clin Epigenetics 2021;13:65.
30. Alashkar Alhamwe B, Alhamdan F, Ruhl A, Potaczek DP, Renz H. The role of epigenetics in allergy and asthma development. Curr Opin Allergy Clin Immunol 2020;20:48-55.
31. Alaskhar Alhamwe B, Khalaila R, Wolf J, von Bülow V, Harb H, Alhamdan F, et al. Histone modifications and their role in epigenetics of atopy and allergic diseases. Allergy Asthma Clin Immunol 2018;14:39.
32. Zhang X, Ouyang S, Kong X, Liang Z, Lu J, Zhu K, et al. Catalytic mechanism of histone acetyltransferase p300: from the proton transfer to acetylation reaction. J Phys Chem B 2014;118:2009-19.
33. Ito K, Caramori G, Lim S, Oates T, Chung KF, Barnes PJ, et al. Expression and activity of histone deacetylases in human asthmatic airways. Am J Respir Crit Care Med 2002;166:392-6.
34. Cosío BG, Mann B, Ito K, Jazrawi E, Barnes PJ, Chung KF, et al. Histone acetylase and deacetylase activity in alveolar macrophages and blood mononocytes in asthma. Am J Respir Crit Care Med 2004;170:141-7.
35. Boonpiyathad T, Sözener ZC, Akdis M, Akdis CA. The role of Treg cell subsets in allergic disease. Asian Pac J Allergy Immunol 2020;38:139-49.
36. Larché M. Regulatory T cells in allergy and asthma. Chest 2007;132:1007-14.
37. Chapoval S, Dasgupta P, Dorsey NJ, Keegan AD. Regulation of the T helper cell type 2 (Th2)/T regulatory cell (Treg) balance by IL-4 and STAT6. J Leukoc Biol 2010;87:1011-8.
38. Floess S, Freyer J, Siewert C, Baron U, Olek S, Polansky J, et al. Epigenetic control of the foxp3 locus in regulatory T cells. PLoS Biol 2007;5:e38.
39. Harb H, Raedler D, Ballenberger N, Böck A, Kesper DA, Renz H, et al. Childhood allergic asthma is associated with increased IL-13 and FOXP3 histone acetylation. J Allergy Clin Immunol 2015;136:200-2.
40. Qiu H, He Y, Ouyang F, Jiang P, Guo S, Guo Y. The Role of Regulatory T Cells in Pulmonary Arterial Hypertension. J Am Heart Assoc 2019;8:e014201.
41. Kim BH, Shenoy AR, Kumar P, Bradfield CJ, MacMicking JD. IFN-inducible GTPases in host cell defense. Cell Host Microbe 2012;12:432-44.
42. Yu X, Jin J, Zheng Y, Zhu H, Xu H, Ma J, et al. GBP5 drives malignancy of glioblastoma

via the Src/ERK1/2/MMP3 pathway. Cell Death Dis 2021;12:203.

43. Li X, Song D, Su S, He X, Cao F, Yang C, et al. Critical role of guanylate binding protein 5 in tumor immune microenvironment and predictive value of immunotherapy response. Front Genet 2022;13:984615.

44. Pfoertner S, Jeron A, Probst-Kepper M, Guzman CA, Hansen W, Westendorf AM, et al. Signatures of human regulatory T cells: an encounter with old friends and new players. Genome Biol 2006;7:R54.

45. Seumois G, Ramírez-Suástegui C, Schmiedel BJ, Liang S, Peters B, Sette A, et al. Single-cell transcriptomic analysis of allergen-specific T cells in allergy and asthma. Sci Immunol 2020;5.

46. Lee SY, Park SY, Lee SH, Kim H, Kwon JH, Yoo JY, et al. The deubiquitinase UCHL3 mediates p300-dependent chemokine signaling in alveolar type II cells to promote pulmonary fibrosis. Exp Mol Med 2023;55:1795-805.

47. Cai Z, Xie Q, Hu T, Yao Q, Zhao J, Wu Q, et al. S100A8/A9 in Myocardial Infarction: A Promising Biomarker and Therapeutic Target. Front Cell Dev Biol 2020;8:603902.

48. Ozga AJ, Chow MT, Luster AD. Chemokines and the immune response to cancer. Immunity 2021;54:859-74.

49. Lv M, Xu Y, Tang R, Ren J, Shen S, Chen Y, et al. miR141-CXCL1-CXCR2 signaling-induced Treg recruitment regulates metastases and survival of non-small cell lung cancer. Mol Cancer Ther 2014;13:3152-62.

Abstract in Korean

알레르기성 천식에서 EP300이 조절 T 세포에 미치는 영향

배경: 천식은 만성 염증성 기도 질환으로 후성유전학적 변형인 히스톤 아세틸화를 통해 조절될 수 있다. 히스톤 아세틸화를 조절하는 중요한 히스톤 아세틸전달효소 중 하나인 E1A binding protein p300 (EP300)은 세포 증식 및 염증성 유전자 발현을 포함한 다양한 세포 기능에 필수적이라고 알려져 있다. 따라서 본 연구에서는 천식 발병기전에서 EP300의 역할을 규명해 보고자 한다.

방법: 전신 EP300 결실 마우스와 조절 T 세포 특이적 EP300 결실 마우스에 난백알부민 혹은 집먼지진드기를 이용하여 천식 모델을 확립하였다. 천식이 유발된 마우스에 히스톤 아세틸전달효소 활성과 EP300 발현을 확인하였다. 또한, 천식 환자 및 대조군의 폐 생검에서 EP300 발현을 평가하였다. 다음으로 제2형 도움 T 세포와 조절 T 세포의 면역반응을 비교하였고, 분화 및 억제 실험을 통한 조절 T 세포의 기능적 연구를 수행하였다. 이후, 조절 T 세포를 분리하여 염색질 면역침전 시퀀싱 및 RNA 시퀀싱을 진행하였고, EP300 억제제와 guanylate binding protein 5 (GBP5) 간섭 RNA 및 GBP5 과발현 벡터를 사용하여 조절 T 세포 증식 실험을 수행하였다.

결과: 본 연구에서는 히스톤 아세틸전달효소 활성과 EP300의 발현이 천식이 유발된 마우스에서 현저히 증가한 것을 확인하였다. 또한, EP300 발현은 정상 대조군에 비해 천식 환자에서 더 높은 것을 확인하였다. 천식이 유도된 전신 EP300 결실 마우스는 대조군 마우스에 비해 기도 과민반응이 증가하고, 염증 세포 수, IgE 발현량, 제2형 사이토카인 발현 및 폐 조직 염증의 중증도가 높은 것을 확인하였다. 그러나 조절 T 세포 관련 유전자의 발현과 조절 T 세포의 수는 대조군 마우스보다 EP300 결실 마우스에서 유의하게 감소했다. 추가로 조절 T 세포에 관한 기능적 연구를 통해 EP300 결실이 조절 T 세포의 억제

능력과 분화 잠재력을 감소시키는 것으로 나타났다. 전신 EP300 결실 마우스와 유사하게, 천식이 유도된 조절 T 세포 특이적 EP300 결실 마우스에서도 대조군 마우스보다 더욱 악화된 알레르기 염증 반응을 보였다. 마지막으로 염색질 면역침전 시퀀싱 및 RNA 시퀀싱을 통해 천식 유발 시 조절 T 세포에서 *GBP5*가 EP300의 중요한 표적 유전자임을 확인하였고, 조절 T 세포 증식 실험을 통해 EP300이 GBP5를 활성화함으로써 조절 T 세포의 증식을 유도한다는 것을 밝혔다.

결론: 본 연구에서는 EP300이 조절 T 세포를 제어함으로써 알레르기 염증 반응을 조절한다는 것을 입증하였다. 이러한 연구 결과는 천식 진단 및 치료에 대한 새로운 접근 방식을 개발하는 데 도움이 될 수 있을 것이다.

핵심되는 말 : 천식, GBP5, EP300, 조절 T 세포, 제2형 도움 T 세포